4th Japan-Korea Joint Symposium on
Plasma and Electrostatics Technologies for Environmental Application
Dec. 10-11.2015, Kyoto, Japan

Hydrogen production from ammonia by DBD pulsed plasma with hydrogen permeable membrane

Prof. Shinji Kambara

Gifu University, JAPAN
Graduate School of Engineering,
Energy and Renewable Energy System Division

Background

To promote hydrogen economy, ammonia (NH_3) is expected as hydrogen carrier and hydrogen storage materials.

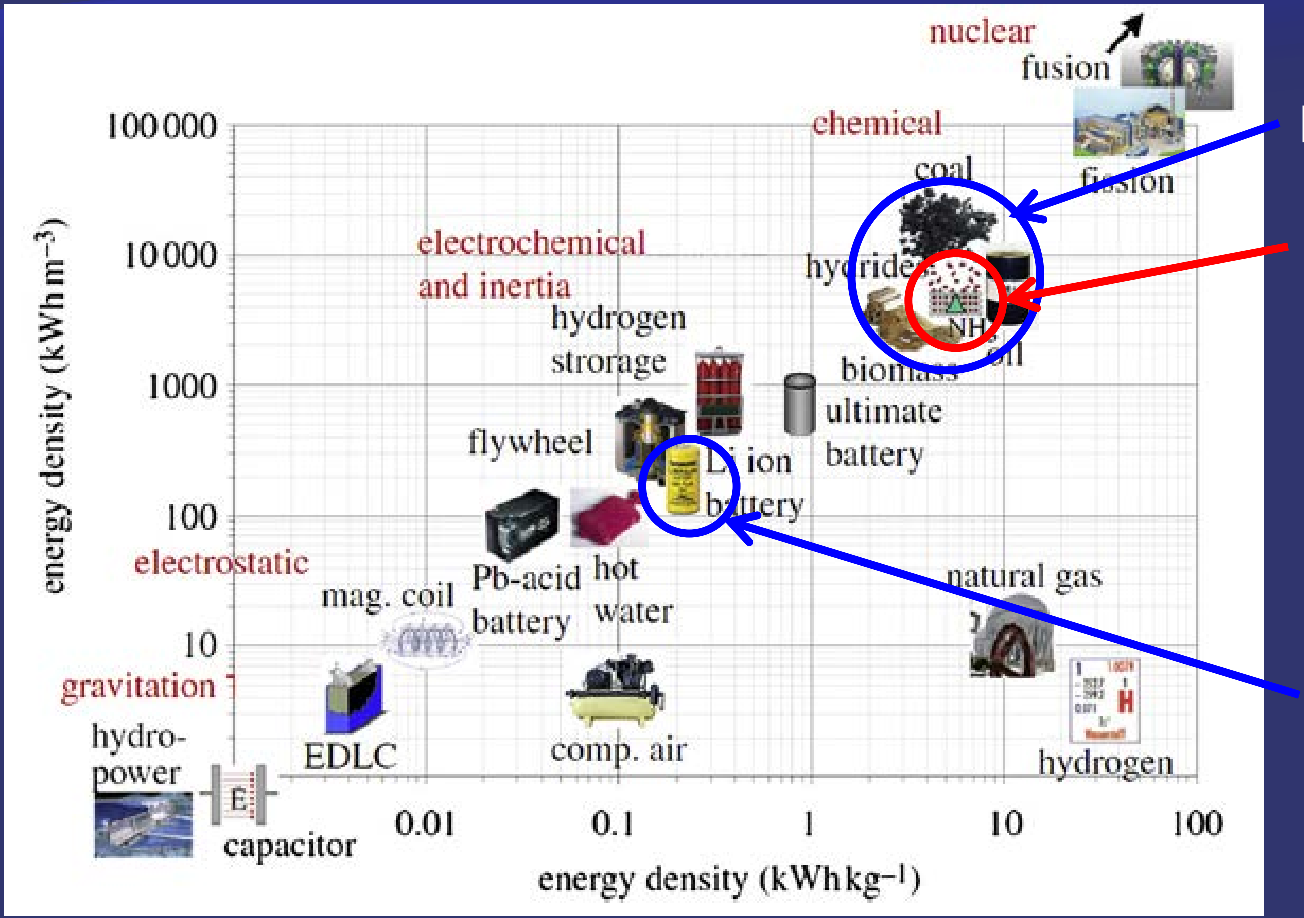

Fossil fuels

Ammonia

$$\frac{H_3}{NH_3} = 17.6\%$$

Li-ion
battery

Fig. 1 Energy density (kWh/kg vs. kWh/m^3) of various materials.

Typical Energy Carrier & Storage System

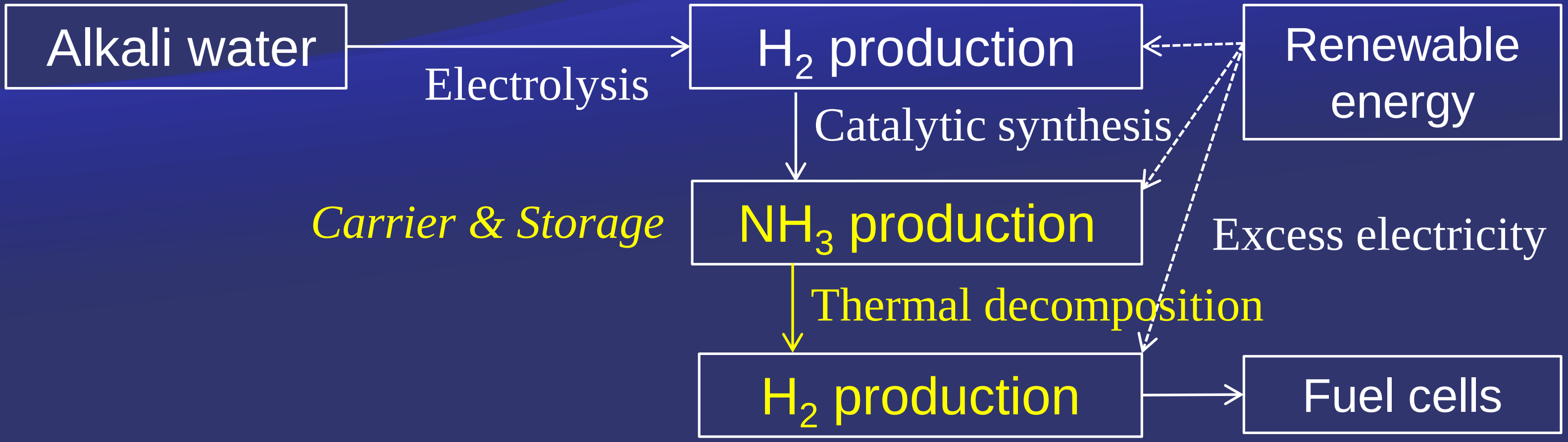

Alkali water

Electrolysis

H_2 production

Catalytic synthesis

Renewable energy

Carrier & Storage

NH_3 production

Excess electricity

Thermal decomposition

H_2 production

Fuel cells

Fig.2 Typical hydrogen energy carrier and storage system incorporating renewable energy systems

This system has:

1) hydrogen production by electrolysis of alkali water,
2) ammonia production by synthesis of hydrogen and nitrogen,
3) hydrogen production by ammonia decomposition.

Proposed Energy Carrier & Storage System

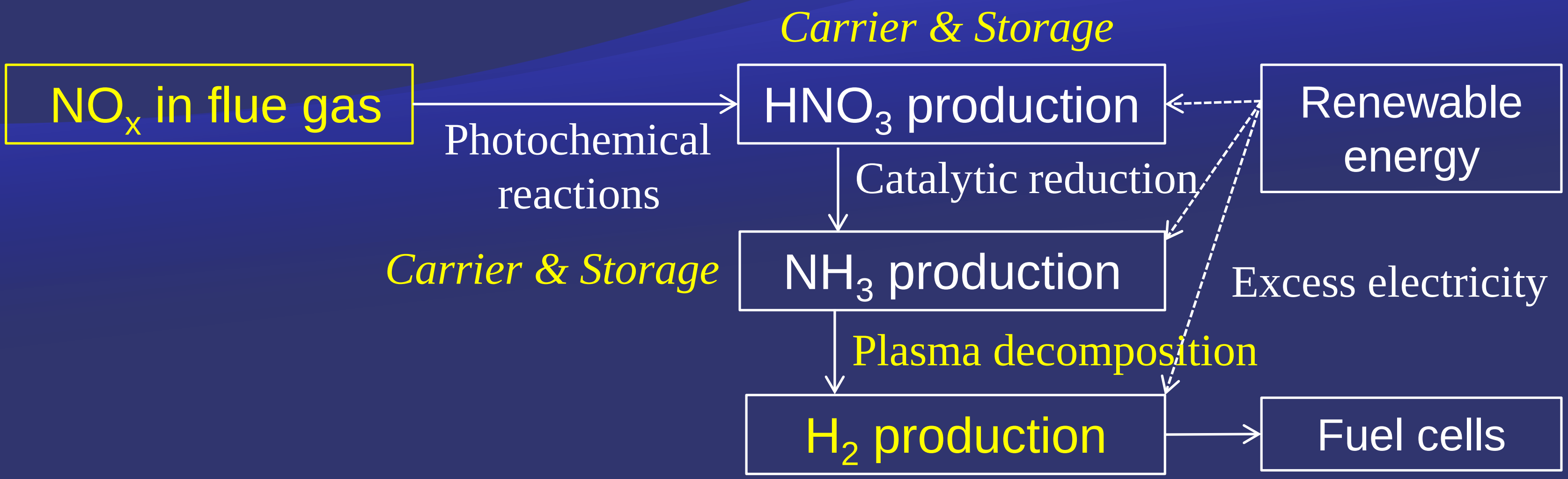

Carrier & Storage

NO_x in flue gas

Photochemical reactions

HNO_3 production

Renewable energy

Catalytic reduction

Carrier & Storage

NH_3 production

Excess electricity

Plasma decomposition

H_2 production

Fuel cells

Fig.3 Proposed energy carrier and storage system.

This system has:

1) nitric acid production from NO_x by photochemical reactions,
2) ammonia production from HNO_3 by reduction,
3) hydrogen production by ammonia decomposition.

Objectives

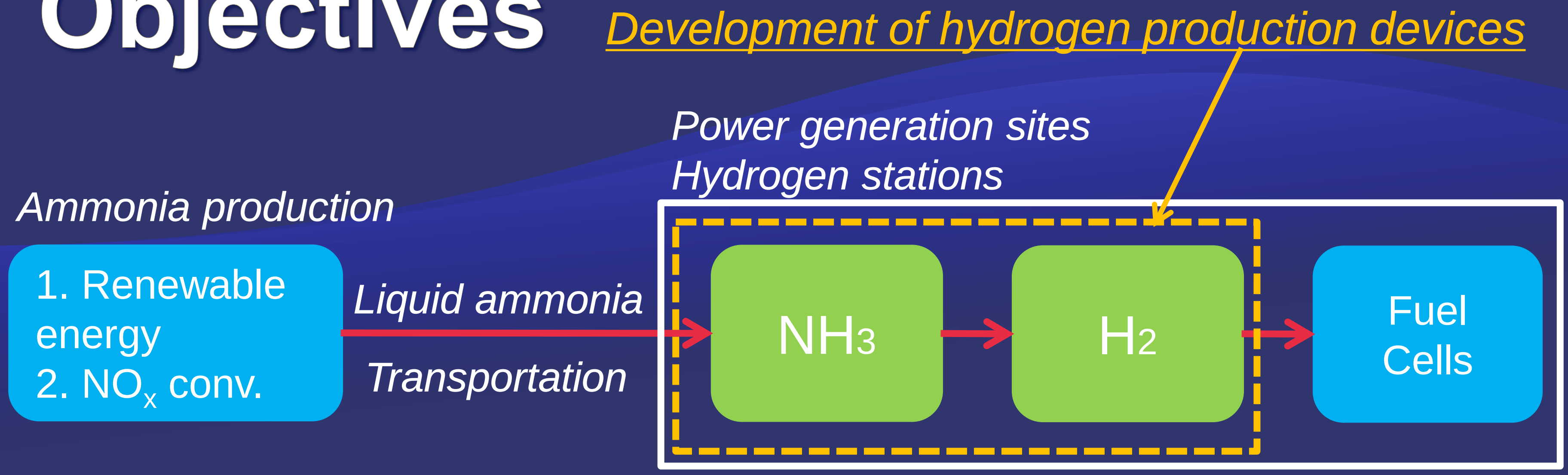

Fig. 4 Key technology for hydrogen carrier and storage system.

Technical issues

1. High energy efficiency for H_2 production.
2. Production of high purity H_2 of 99.9999% for fuel cells.

Plasma techniques may be one of the solution for the issues.

Topics

1. Hydrogen production from ammonia by a DBD pulsed plasma.

2. Reaction mechanism of hydrogen production in the plasma.

3. High purity hydrogen production by the DBD pulsed plasma with hydrogen separation membrane.

Experimental Setup (No membrane)

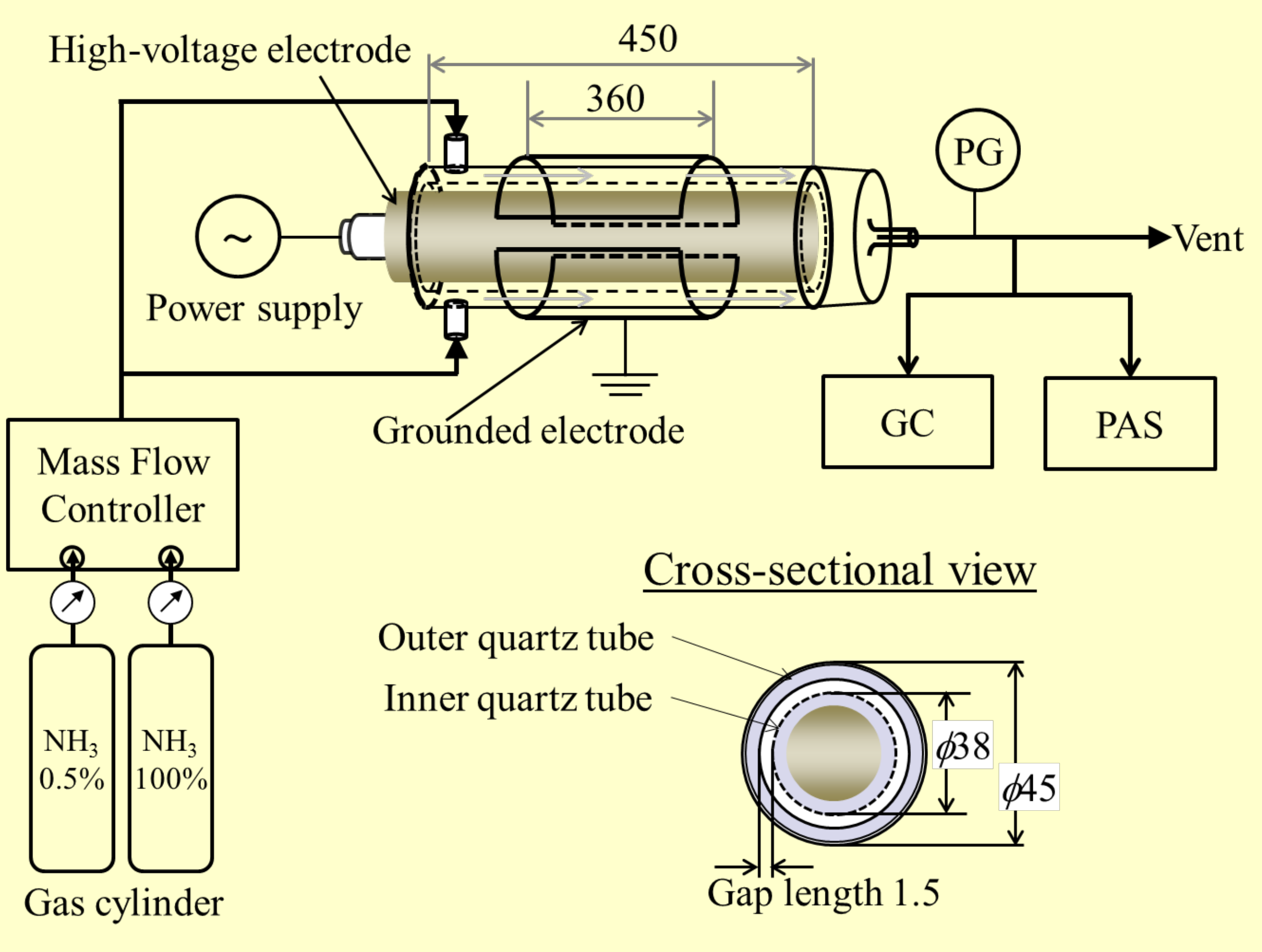

Gas analyzers

1) For N_2 and H_2 measurement
   Micro GC (Agilent 300A):
   - Porapack Q capillary column
   - TCD
2) For NH_3 measurement
   photo acoustic spectroscopy (Gasera Inc., F10):
   - Atmospheric gas
   - Continuous measurement

Fig.5 Experimental setup for hydrogen production tests.

Ammonia plasma

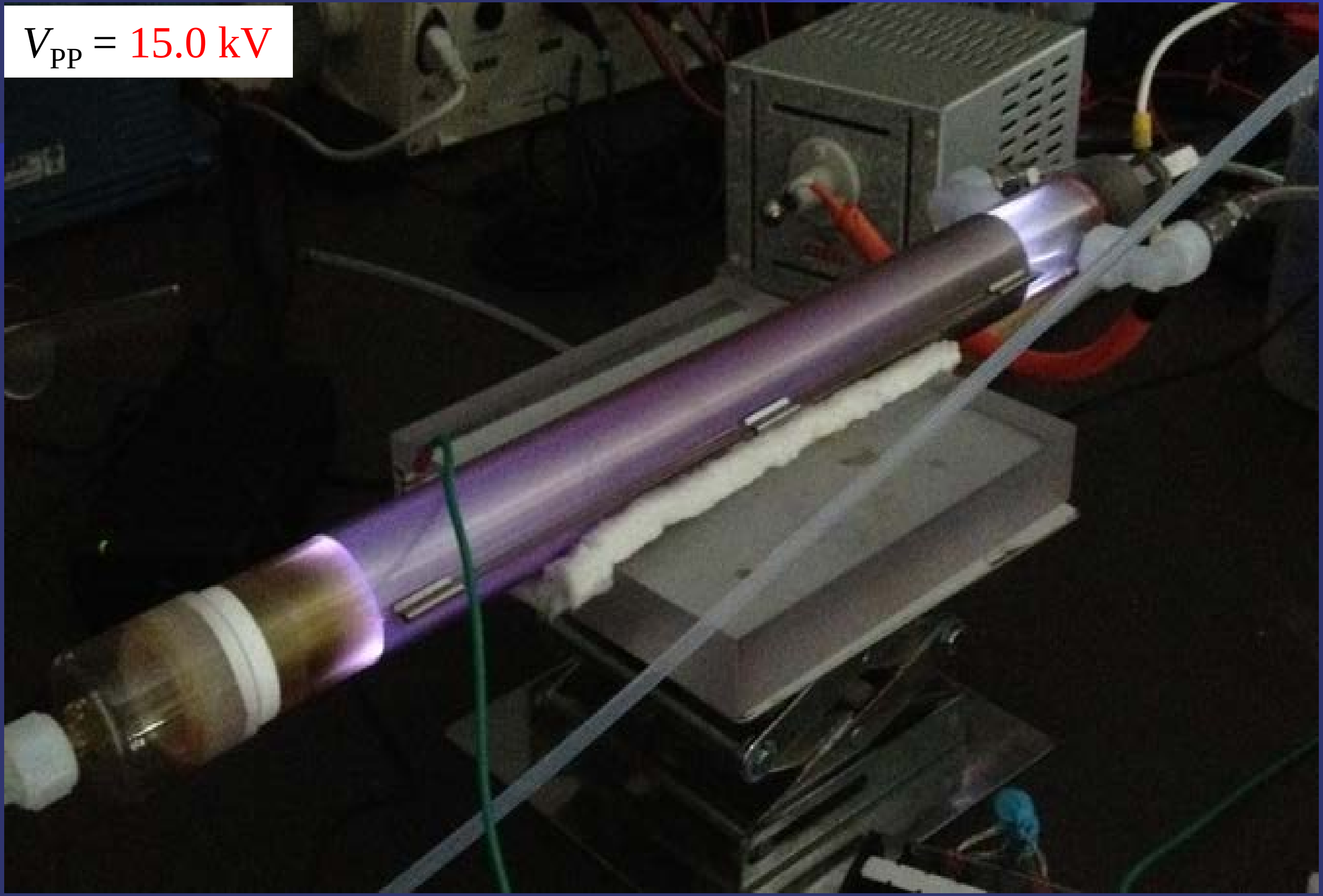

Fig.6 The state of plasma at V_{pp} =15 kV (0.5% NH_3).

Waveforms of the power source

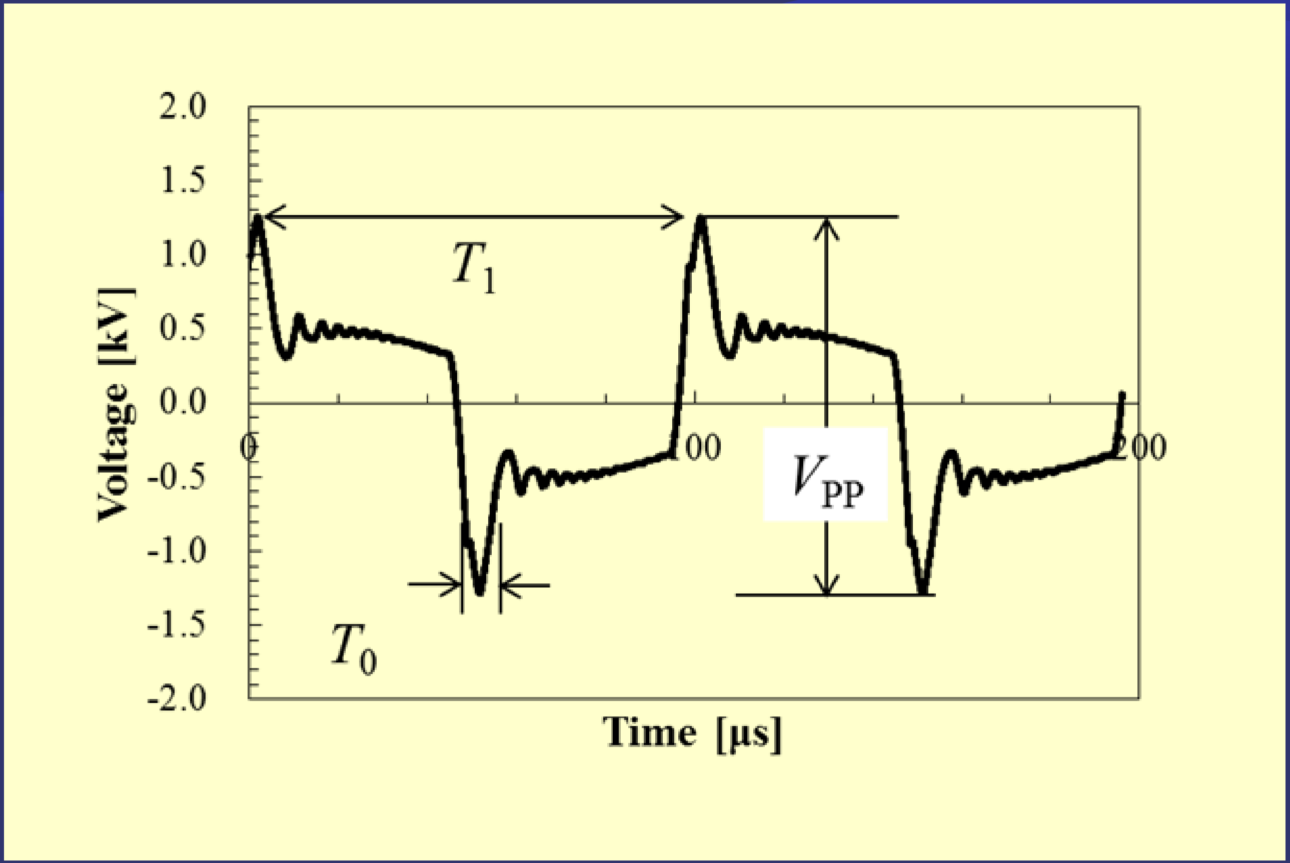

Fig. 7 Waveforms of voltage of the power source.

T_0 : Duration time of one cycle = 10 μs
R_R: Repetition rate = $1/T_0$ = 10kHz
V_{pp} : Applied voltage

Experimental conditions

Table 1 Experimental conditions for H_2 production tests for $0.5\%\ NH_3/Ar$ gas

	Unit	
Repetition rate, R_R	[kHz]	10
Applied voltage, V_{PP}	[kV]	3.5–15
NH_3 conc. (Ar base)	[%]	0.5
Flow rate	[L/min]	0.2–2.0

Overall reactions: $NH_3 + e \rightarrow 0.5\ N_2 + 1.5\ H_2$

Characteristics of H_2 production

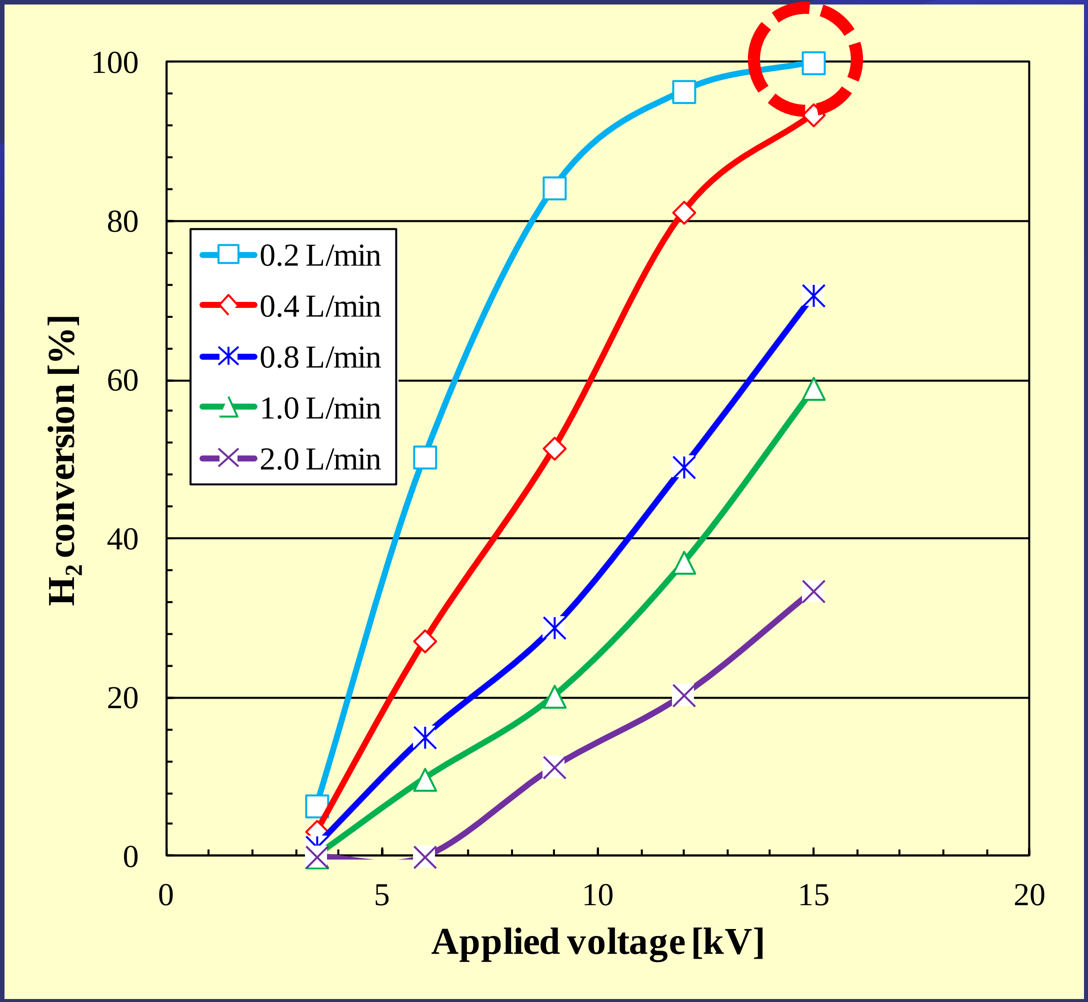

1) H_2 conversion increased with an increase of V_{pp} , and decreased with an increase of NH_3 flow rate.

2) About 100% H_2 conversion was attained at V_{pp} = 15 kV and F = 0.2 L/min.

Fig.8 Effects of applied voltage and flow rates of 0.5% NH_3 on H_2 conversion.

Detailed chemical compositions

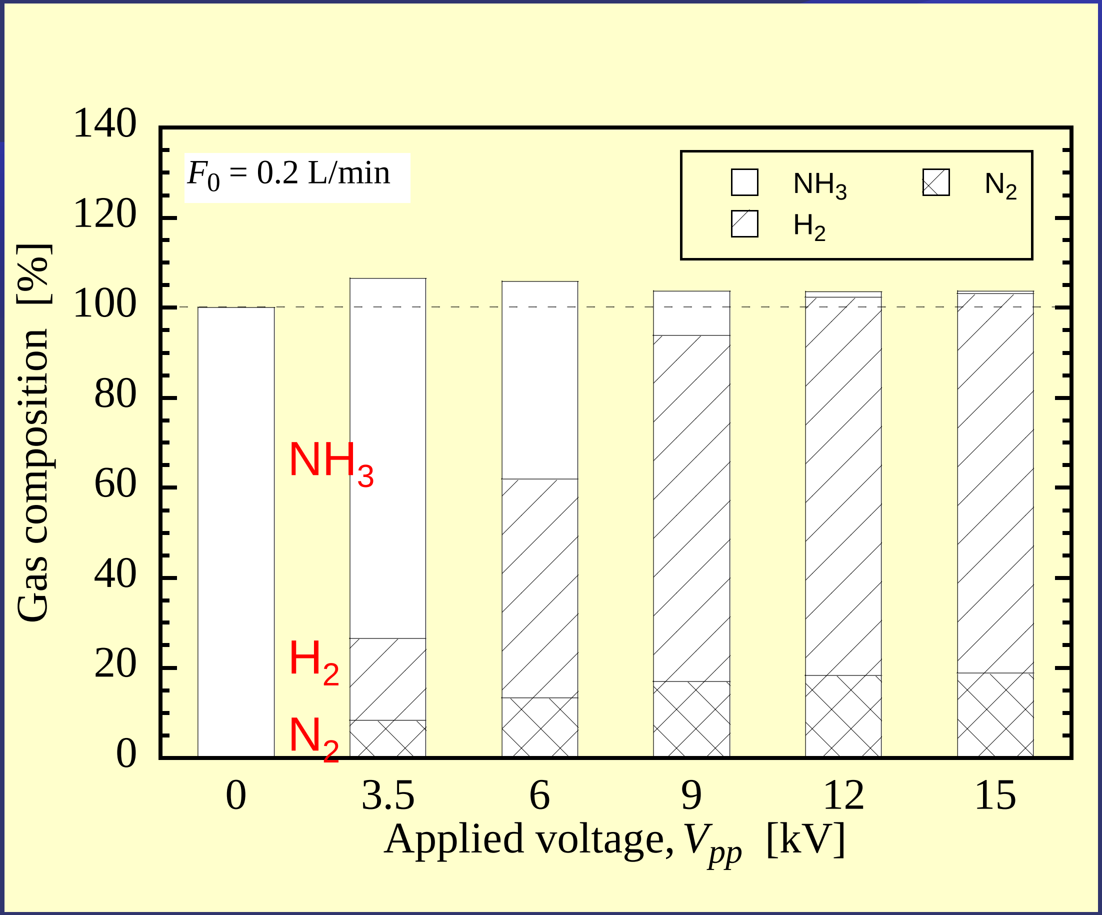

1) Detected chemical species were H_2, N_2, and unreacted NH_3. H_2 fraction increased with an increase of V_{pp}.

2) At 15 kV, unreacted NH_3 conc. was about 300 ppm. (H_2 conversion: 99.97%)

⇩

This is “No Good” result. The limitation of NH_3 conc. for FC is below 0.1 ppm !

Fig.9 Chemical composition at various applied voltages (NH_3 = 0.5, the flow rate = 0.2 L/min).

Energy efficiency

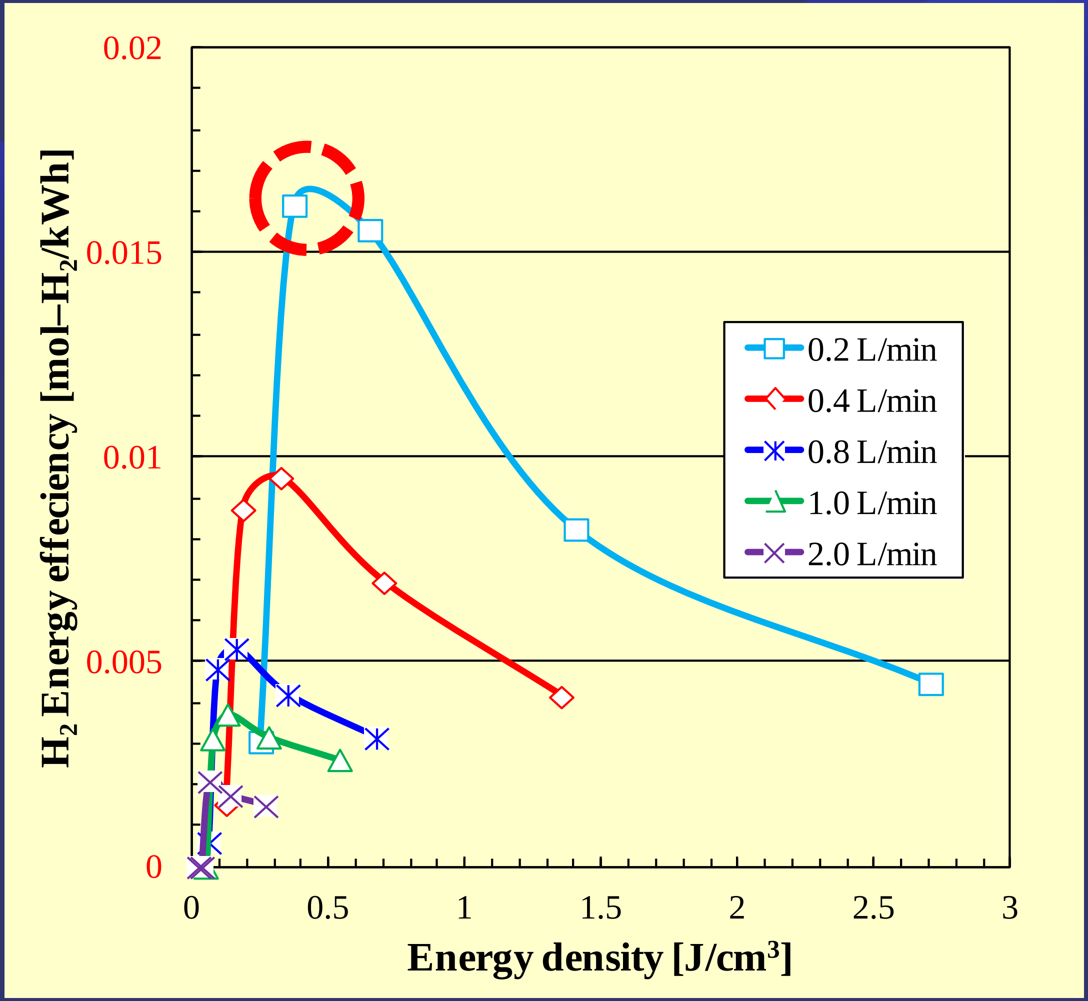

Maximum EE = 0.016 mol-H_2/kWh (0.13%).
But, this is not enough for practical use.

The EE rapidly decreased after the peak value, because NH_3 may be produced by reverse reactions.

Fig.10 Variation in energy efficiency of H_2 production for various V_{pp} and *F*.

Mechanisms of H_2 production

NH_3 decomposition

$\boxed{NH_3} + e \rightarrow N + H + \boxed{H_2} + e$ (2): Low V_{pp}

N_2 production

$N + N \rightarrow \boxed{N_2}$ (3): Low V_{pp}

N_2 and H_2 decomposition

$N + N \leftarrow N_2$ (4): High V_{pp}

$H + H \leftarrow H_2$ (5): High V_{pp}

NH_3 recombination

$N + 3H \rightarrow NH_3$ (6): High V_{pp}

To improve the energy efficiency,

1) High concentration of NH_3 must be used at a low V_{pp}.
2) Generated H radical must be removed from the plasma.

Elemental reaction simulation

CHEMKIN-PRO was used for the simulation

Below models and experimental conditions have to input on CHEMKIN-PRO.

(1) Plasma reactor model
(2) Experimental conditions
(3) Elementary reaction models
- Gas-phase reaction model
- Surface reaction model

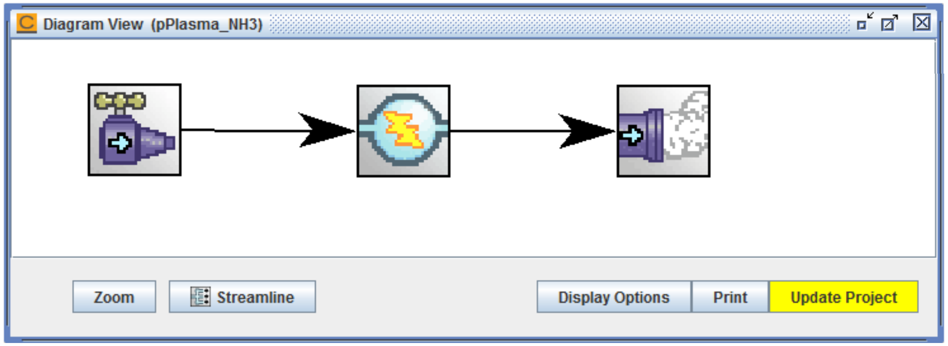

+Reactor volume
+Discharge power
+Inlet gas compositions and the flow rates

Elementary reaction model

◆Electron impact model, Gas-phase reaction model, Surface reaction model were considered as reaction mechanism of NH_3 decomposition in the DBD pulsed plasma.

Table 3 Electron impact model and gas-phase reaction model

R1	$NH_3+H=NH_2+H_2$ 1)	R6	$NH_3+e^-=NH+2H+e^-$ 2)
R2	$NH_3+M=NH_2+H+M$ 1)	R7	$e^-+H_2=2H+e^-$ 2)
R3	$NH+H=N+H_2$ 1)	R8	$NH_3+e^-=NH_3^++2e^-$ 2)
R4	$NH_2+NH=N_2H_2+H$ 1)	R9	$NH_3+e^-=NH_3^-$ 2)
R5	$N_2H_2+H=NNH+H_2$ 1)	R10	$NH_3+e^-=NH+H_2+e^-$ 2)

Ref.
1) Suitable model was applied.
2) Matzing.H: *Adv.Chem.Phys*. (1991)

◆ Bai's Surface reaction model was used.

1. Reactions of positive ions and electrons recombination on the surface.
2. Reactions by adsorption on the surface.

Ref. Bo Bai. An Experimental Study and Modeling of Transformer-Coupled Toroidal Plasma processing of Materials. (2006)

Applied gas phase reaction model

GIFU UNIVERSITY

Which are gas-phase reaction models suitable for the plasma reactions?

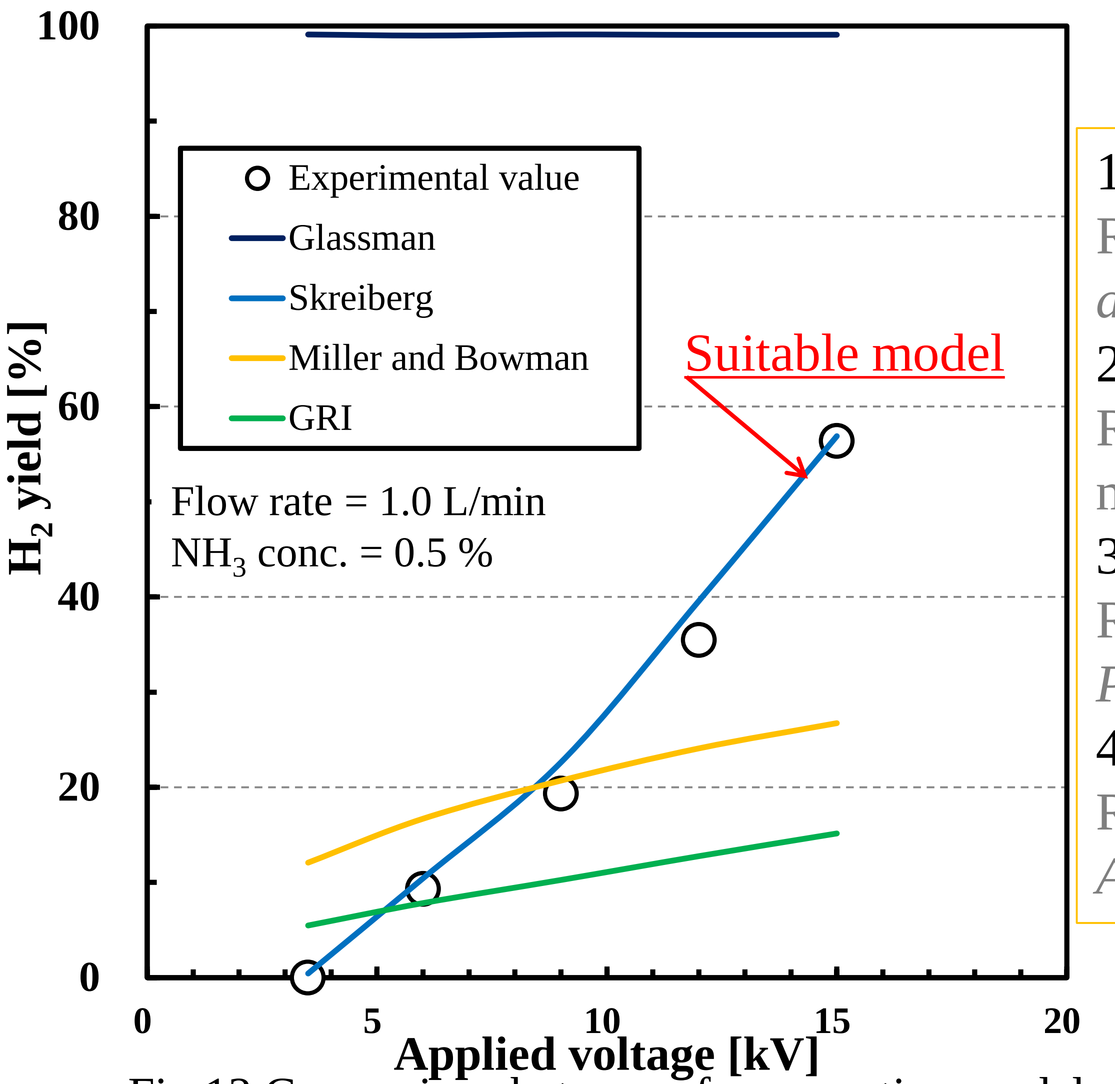

Fig.12 Comparison between four reaction models and experimental value.

4 reaction models

1) Model of Skreiberg et al.
Ref. Skreiberg, Ø. et al, *Combustion and Flame*,(2004)

2) Model of GRI et al.
Ref.wttp://www.me.berkely.edu/gri_mech/

3) Model of Miller and Bowman.
Ref. J.A. Miller and C.T. Bowman, *Prog. Energy Combust. Sci.*, (1989)

4) Model of Glassman et al.
Ref. I. Glassman. *Combustion. Academic Press*, *3rd edition*, (1996).

Detailed gas phase reaction model

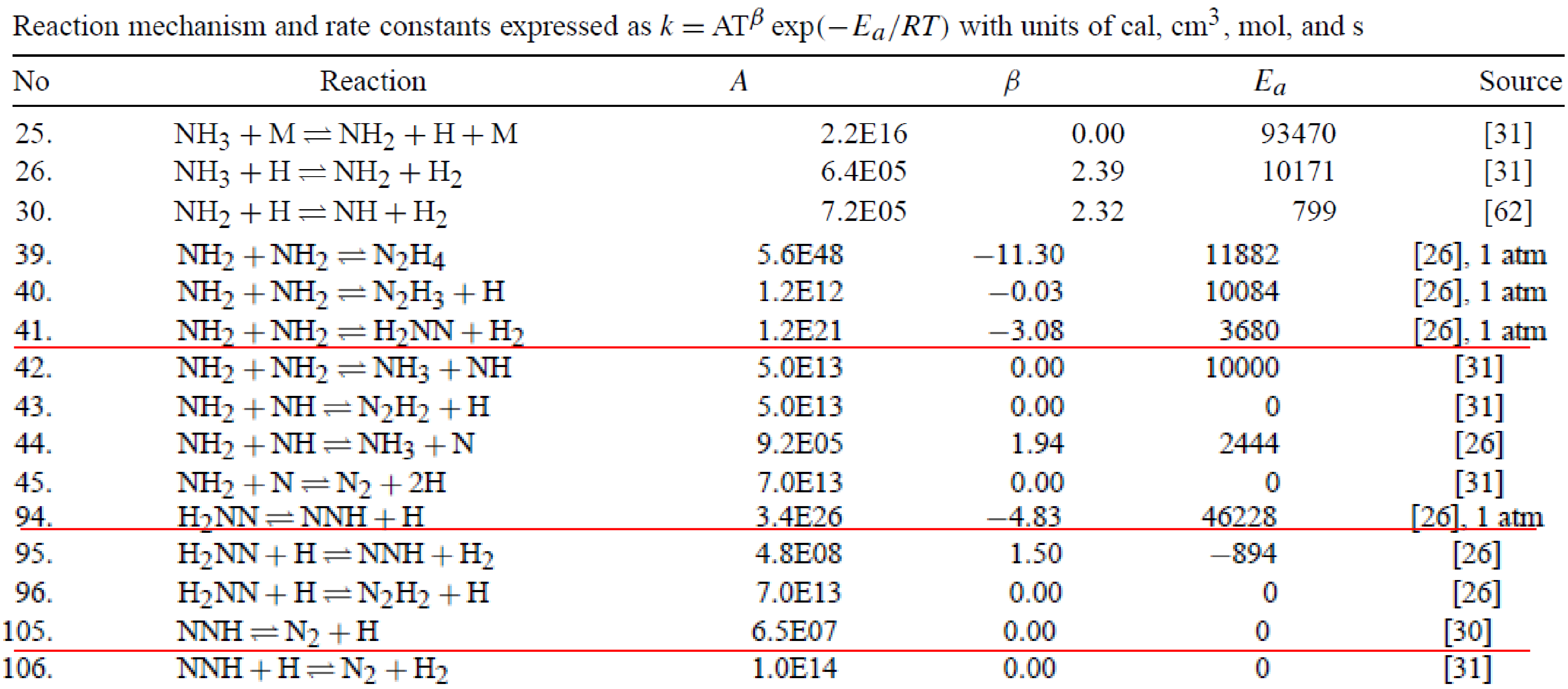

Reaction mechanism and rate constants expressed as $k = \mathrm{A}T^{\beta}\exp(-E_a/RT)$ with units of cal, cm^3, mol, and s

No	Reaction	A	β	E_a	Source
25.	$NH_3 + M \rightleftharpoons NH_2 + H + M$	2.2E16	0.00	93470	[31]
26.	$NH_3 + H \rightleftharpoons NH_2 + H_2$	6.4E05	2.39	10171	[31]
30.	$NH_2 + H \rightleftharpoons NH + H_2$	7.2E05	2.32	799	[62]
39.	$NH_2 + NH_2 \rightleftharpoons N_2H_4$	5.6E48	−11.30	11882	[26], 1 atm
40.	$NH_2 + NH_2 \rightleftharpoons N_2H_3 + H$	1.2E12	−0.03	10084	[26], 1 atm
41.	$NH_2 + NH_2 \rightleftharpoons H_2NN + H_2$	1.2E21	−3.08	3680	[26], 1 atm
42.	$NH_2 + NH_2 \rightleftharpoons NH_3 + NH$	5.0E13	0.00	10000	[31]
43.	$NH_2 + NH \rightleftharpoons N_2H_2 + H$	5.0E13	0.00	0	[31]
44.	$NH_2 + NH \rightleftharpoons NH_3 + N$	9.2E05	1.94	2444	[26]
45.	$NH_2 + N \rightleftharpoons N_2 + 2H$	7.0E13	0.00	0	[31]
94.	$H_2NN \rightleftharpoons NNH + H$	3.4E26	−4.83	46228	[26], 1 atm
95.	$H_2NN + H \rightleftharpoons NNH + H_2$	4.8E08	1.50	−894	[26]
96.	$H_2NN + H \rightleftharpoons N_2H_2 + H$	7.0E13	0.00	0	[26]
105.	$NNH \rightleftharpoons N_2 + H$	6.5E07	0.00	0	[30]
106.	$NNH + H \rightleftharpoons N_2 + H_2$	1.0E14	0.00	0	[31]

◆ H_2NN and NNH chemistry is including in Skreberg’s model.

Simulation results

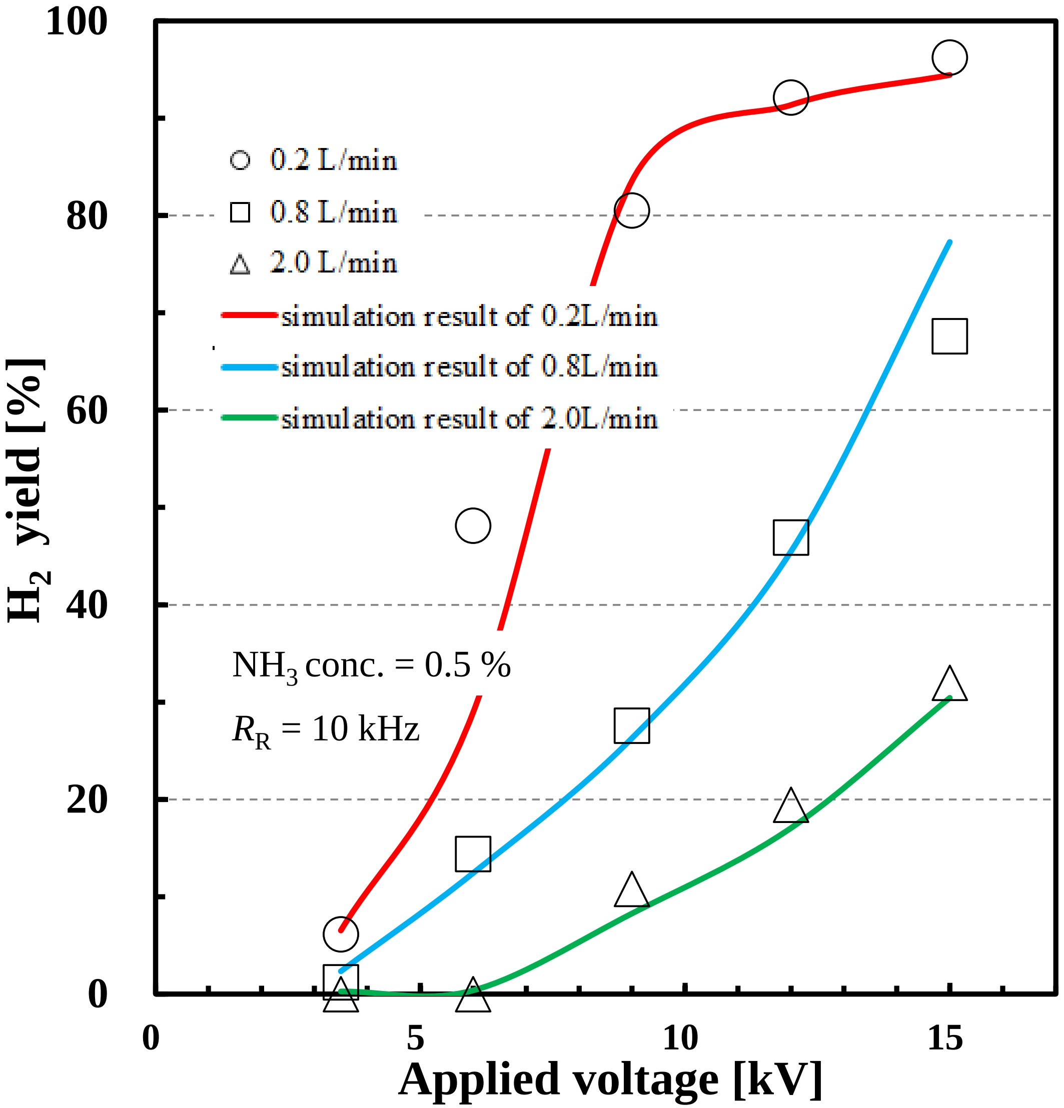

Fig.13 Comparison between simulation results and experimental values.

The simulation results

1) H_2 yield increased with an increase of applied voltage.

2) H_2 yield decreased with an increase of NH_3 flow rate.

The simulation results at different flow rates were agreed with the behavior of the experimental results.

Effect of reverse reactions

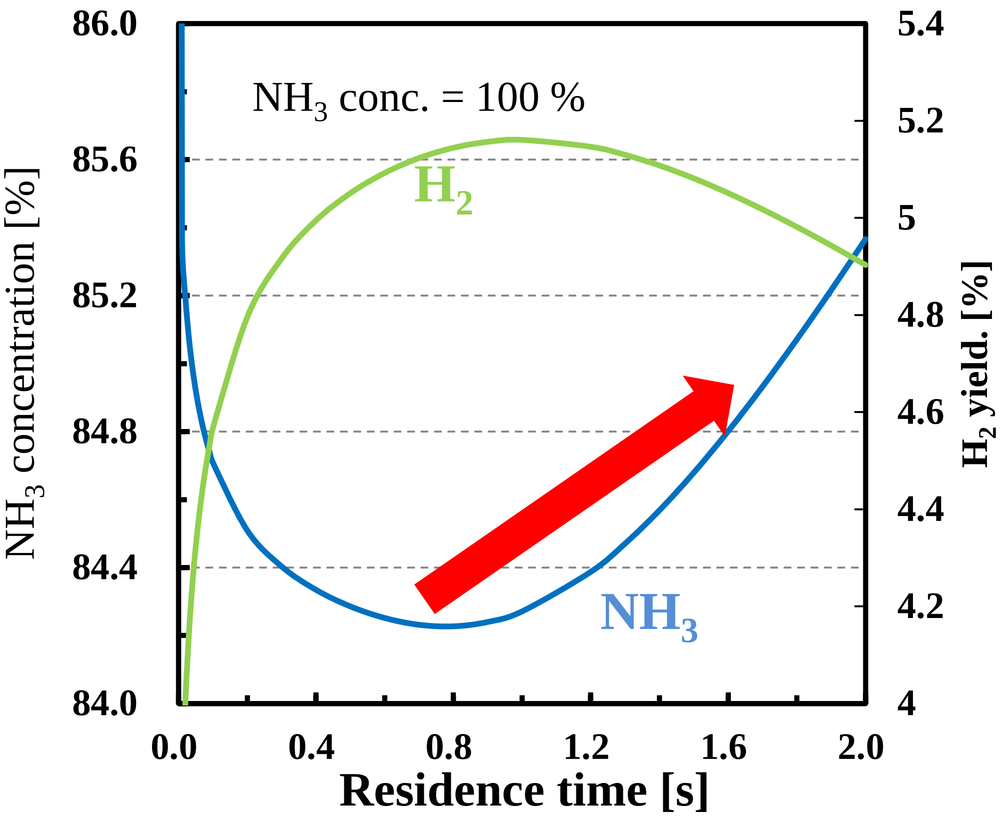

Fig.14 Variation in NH_3 conc. in plasma

NH_3 decomposition and H_2 production

$$NH_3+e \Rightarrow NH+H+H+e$$

$$NH_3+H \Rightarrow NH_2+H_2$$

NH_3 recombination

$$NH_3+e \Leftarrow NH+H_2+e$$

Reverse reaction is occurred in plasma.

H_2 separation membrane

To prevent reverse reactions, hydrogen separation membrane was applied, which is used as a high voltage electrode.

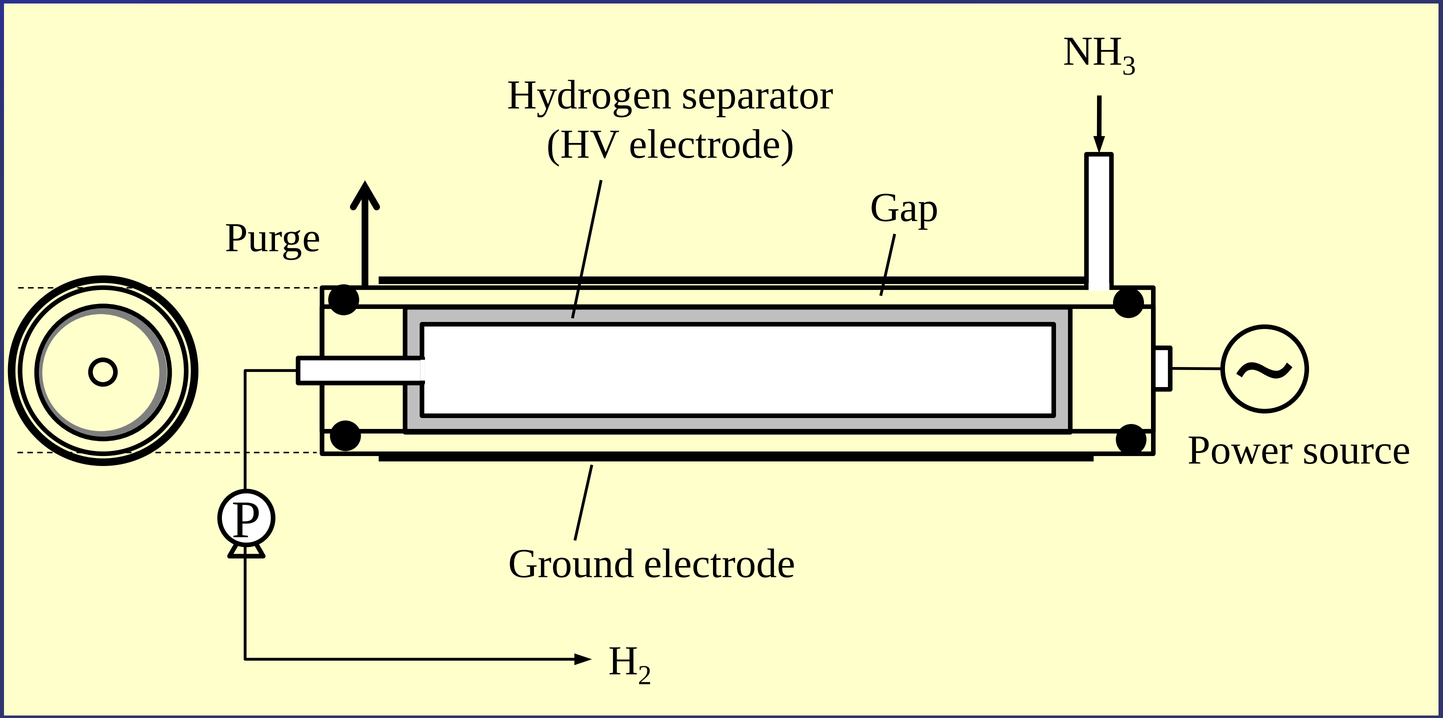

Fig.15 Plasma membrane reactor (PMR). A hydrogen separation membrane was used as the HV electrode.

H_2 separation mechanism

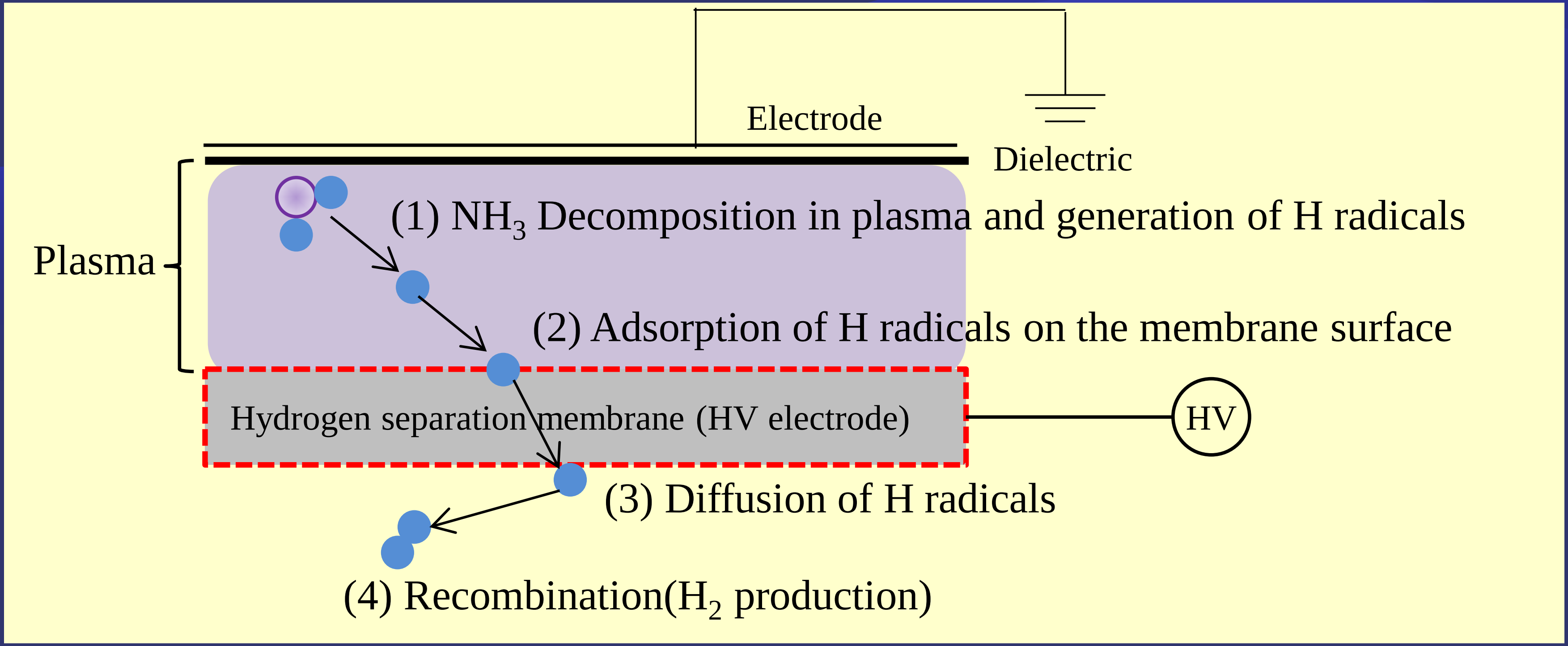

Fig.16 H_2 separation mechanisms in plasma with the hydrogen separation membrane (HSM).

Advantages of the developed plasma device:

1) NH_3 at low temperatures can be used.
2) Produced hydrogen can be used to fuel cells.

Experimental apparatus : Plasma membrane reactor (PMR)

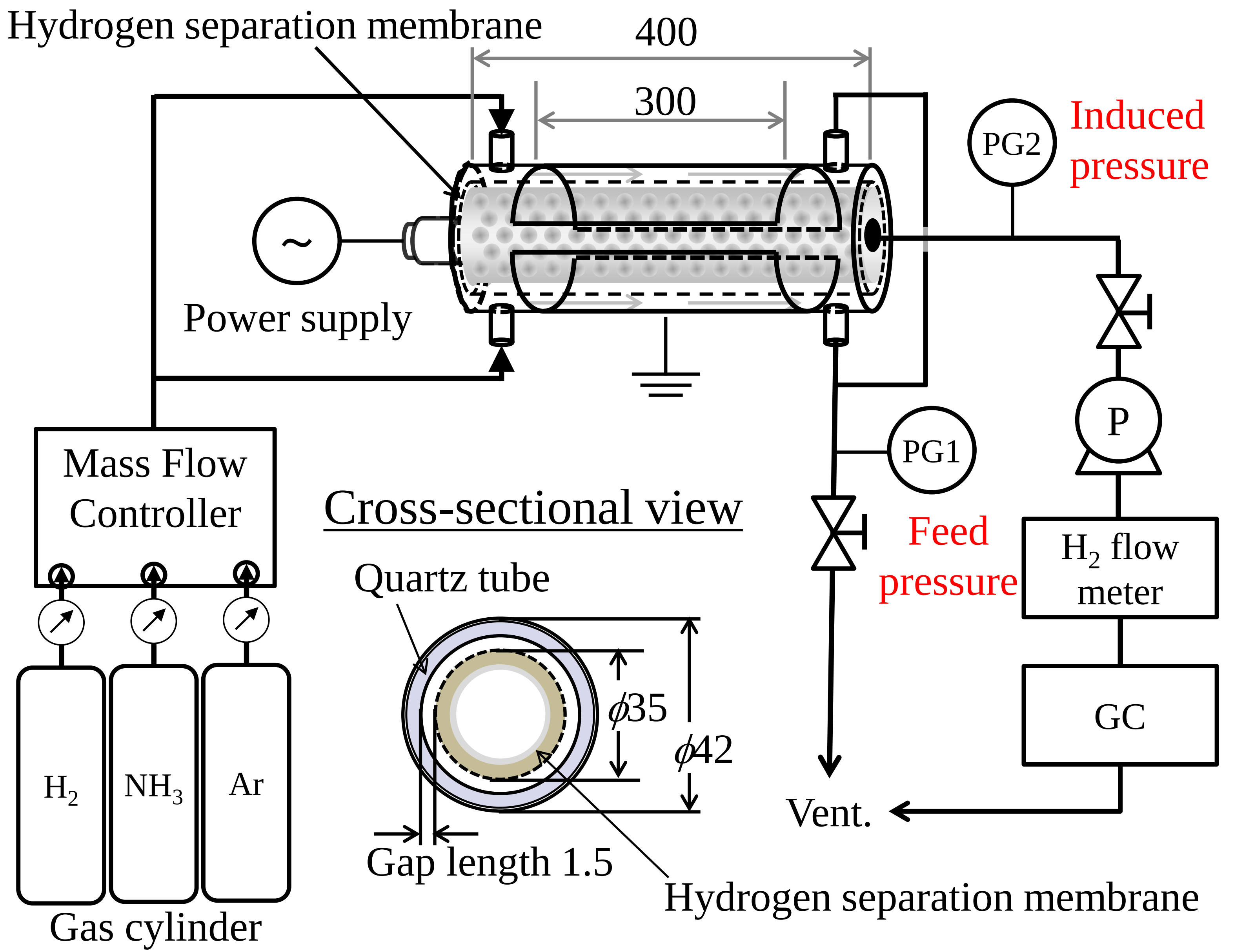

Fig.17 Experimental setup using plasma membrane reactor (PMR).

Experimental equipment: electrode mounted a hydrogen separation membrane

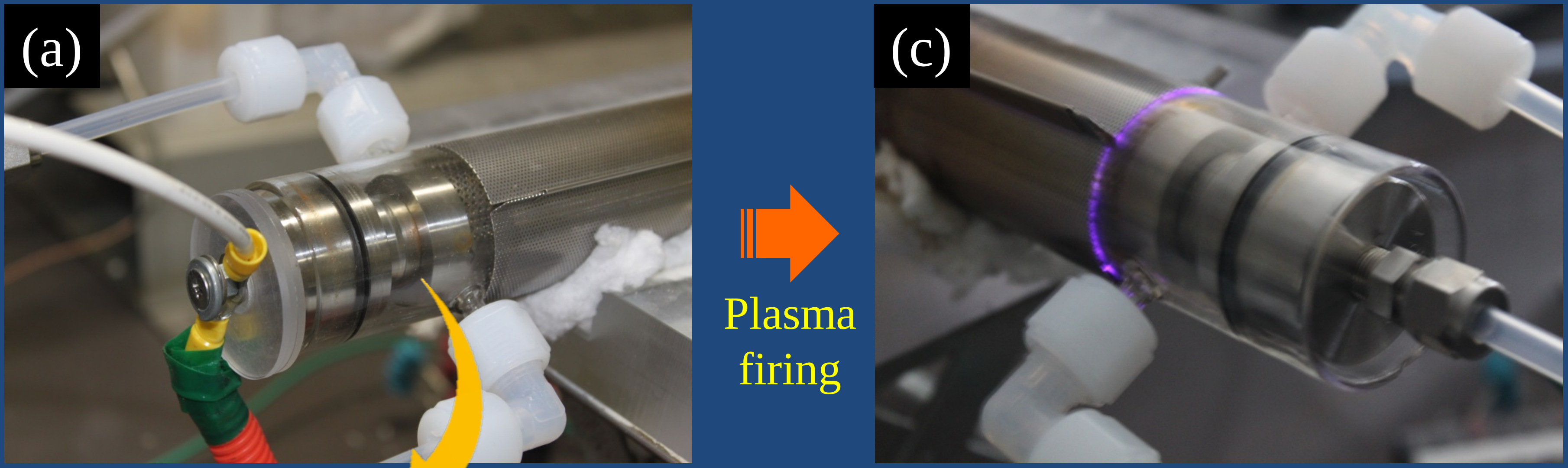

Membrane is welded inside high voltage electrode

Table 1 Specification of hydrogen separation membrane.

	Unit	
Composition ratio	[-]	Pd-40wt%Cu
Thickness	[μm]	20
Limit pressure difference	[kPa]	100

Fig. 18 Plasma membrane reactor. (a) plasma reactor, (b) high voltage electrode with hydrogen separation membrane, (c) condition of plasma firing.

H_2 separation tests by pure H_2

Table Plasma conditions for H_2 separation characteristics tests

Repetition rate, R_{R}	[kHz]	10
Applied voltage, V_{PP}	[kV]	0.0—20.0
Feed pressure, PG_1	[kPa(G)]	0—60
Induced pressure, PG_2	[kPa(G)]	-90—0
H_2 conc. (Ar base)	[%]	10—100
Flow rate	[L/min]	0.5—2.0

H_2 separation characteristics of PMR

Maximum flow rate of the hydrogen separation membrane for the PMR is 48 L/h at ΔP of 70 kPa.

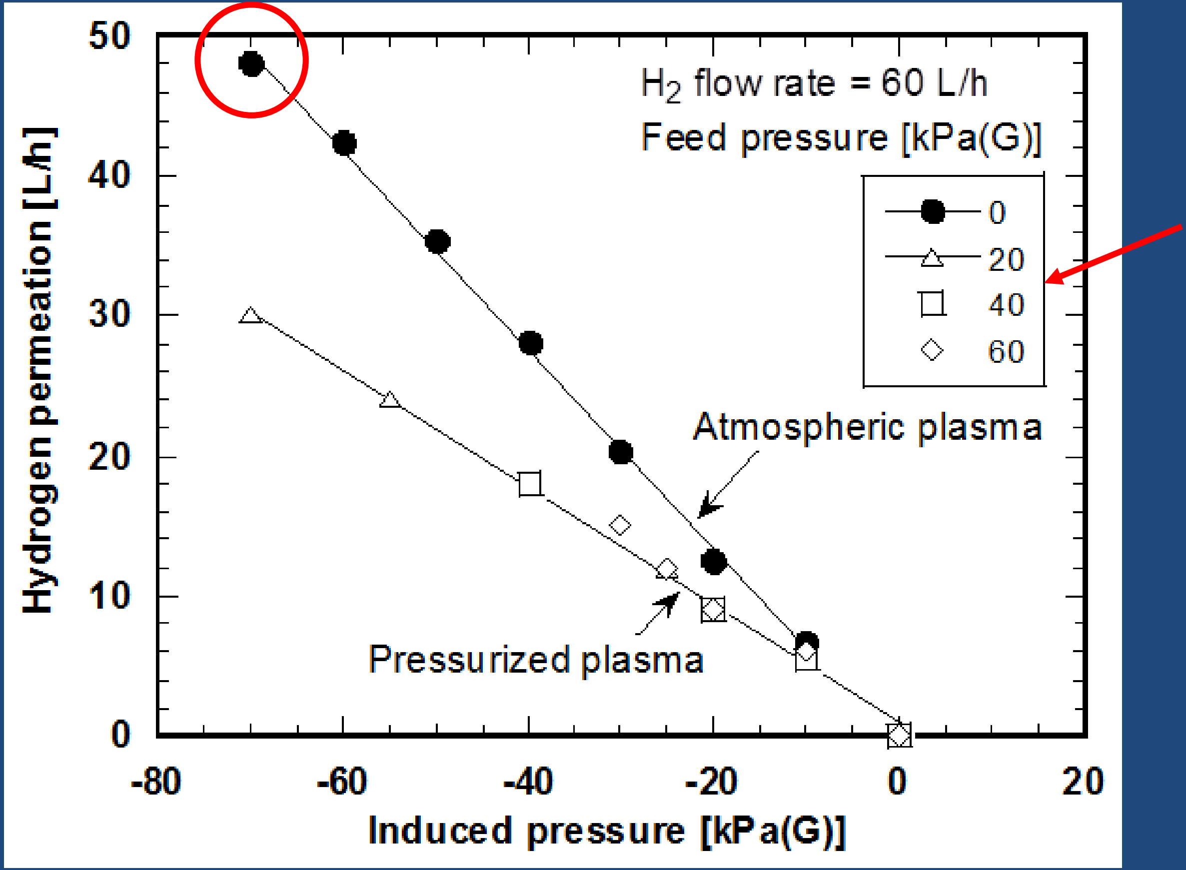

Pressure of PG1

Fig.19 Hydrogen separation characteristics of PMR for pure hydrogen supply

Experimental condition : Hydrogen production experiments with PMR

Hydrogen production experiments were conducted in the PMR using the 100% ammonia gas according to below experimental conditions.

Table 3 Experimental conditions of hydrogen production with PMR.

Repetition rate, R_R	[kHz]	10
Applied voltage, V_{PP}	[kV]	0.0 — 20.0
Pressure of supplied side, P_{G1}	[kPa(G)]	0
Pressure of permeable side, P_{G2}	[kPa(G)]	-90
NH_3 conc.	[%]	100
Flow rate	[L/min]	0.5 — 2.0

Highlights Data:H_2 production by PMR

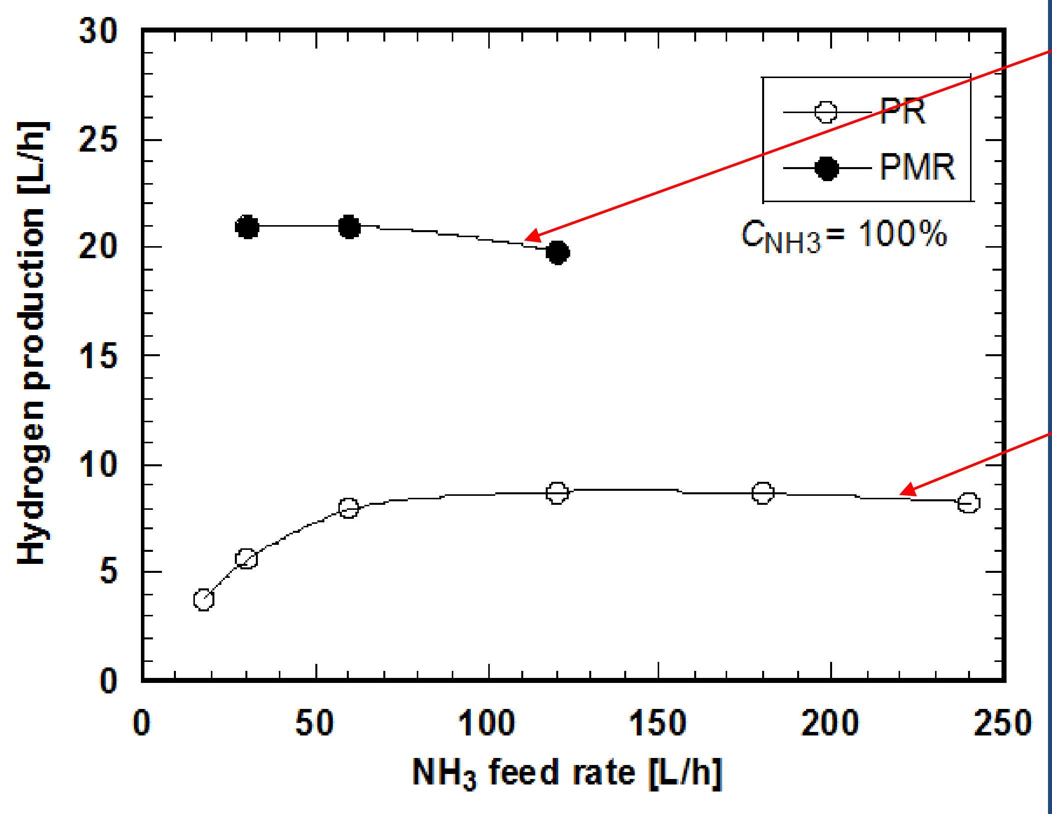

Plasma membrane reactor

H_2 production of 21.0 L/h

EE = 4.42 mol-H_2/kWh

(34.8% at heat value basis)

Pure H_2 of 99.9999%

Plasma reactor

H_2 production of 8.8 L/h

Low EE

Maximum 99.97% H_2

Fig.20 Hydrogen production performance of the PMR and PR using 100% ammonia gas.

Development of energy carrier and storage system

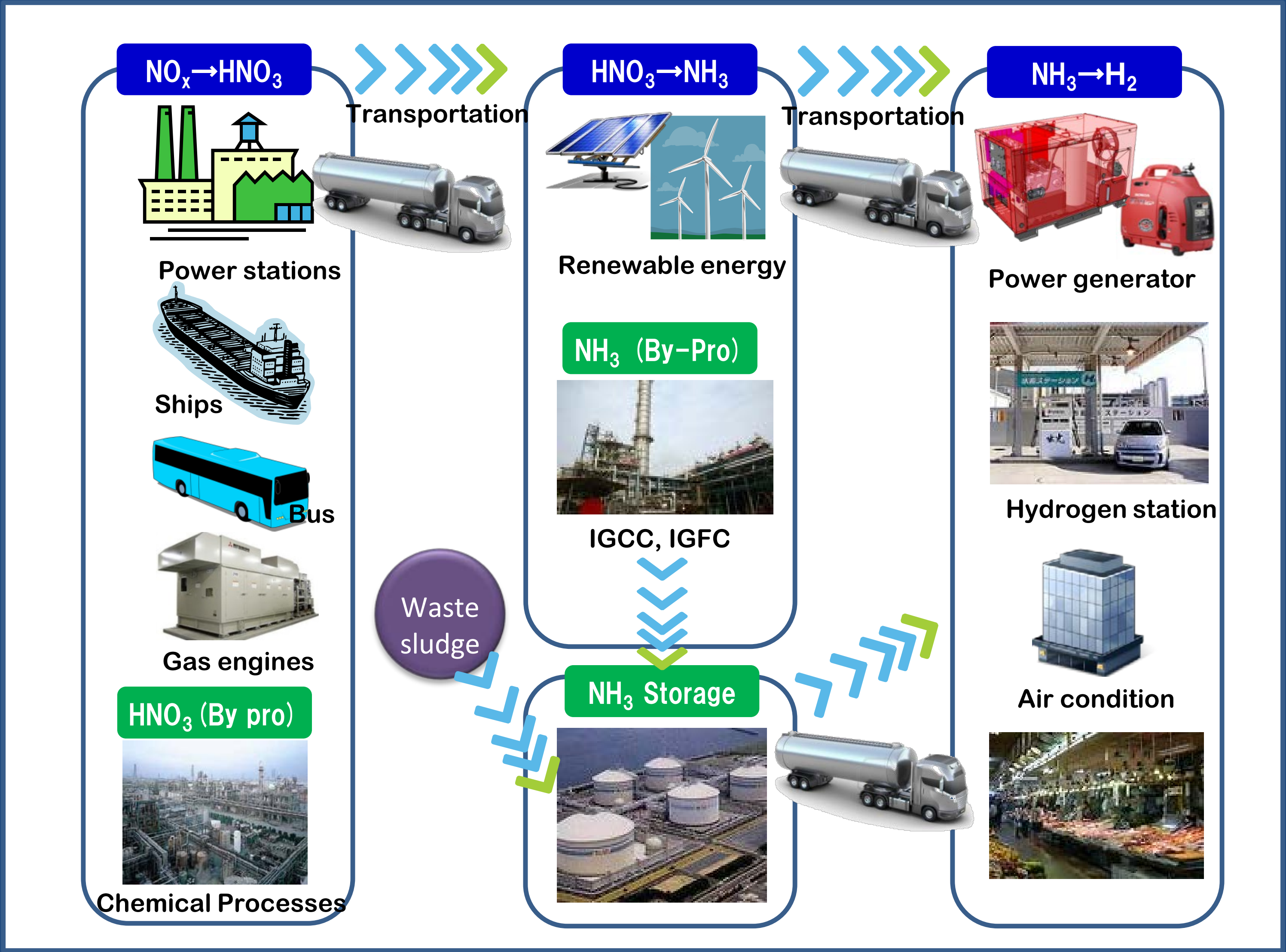

$NO_x \rightarrow HNO_3$

Power stations

Ships

Bus

Gas engines

HNO_3 (By pro)

Chemical Processes

Transportation

$HNO_3 \rightarrow NH_3$

Renewable energy

NH_3 (By-Pro)

IGCC, IGFC

Waste sludge

NH_3 Storage

Transportation

$NH_3 \rightarrow H_2$

Power generator

Hydrogen station

Air condition

Conclusions

1. Hydrogen production from ammonia by a DBD pulsed plasma.

The hydrogen conversion was 99.97% at a flow rate of 0.2 L/min and V_{pp} of 15 kV. However, it was low energy efficiency and no good hydrogen purity for FC.

2. Reaction mechanism of hydrogen production in the plasma.

Ammonia production was occurred by reverse reaction at high applied voltage.

$NH + H_2 + e \rightarrow NH_3 + e$

Reaction mechanism was elucidated by elemental reaction simulation.

3. High purity hydrogen production by the plasma membrane reactor.

The energy efficiency was 4.42 mol-H_2/kWh, which is corresponding to 34.8% energy efficiency based on heat value. Hydrogen purity was good for fuel cells. However, more improvement of energy efficiency is desired for hydrogen carrier and storage system.

Conversion of nitric oxide to HNO_3 at room temperature by VUV radiation

Shinji Kambara

Gifu University, JAPAN
Graduate School of Engineering,
Energy and Renewable Energy Systems Division

Proposed Energy Storage & Carrier System

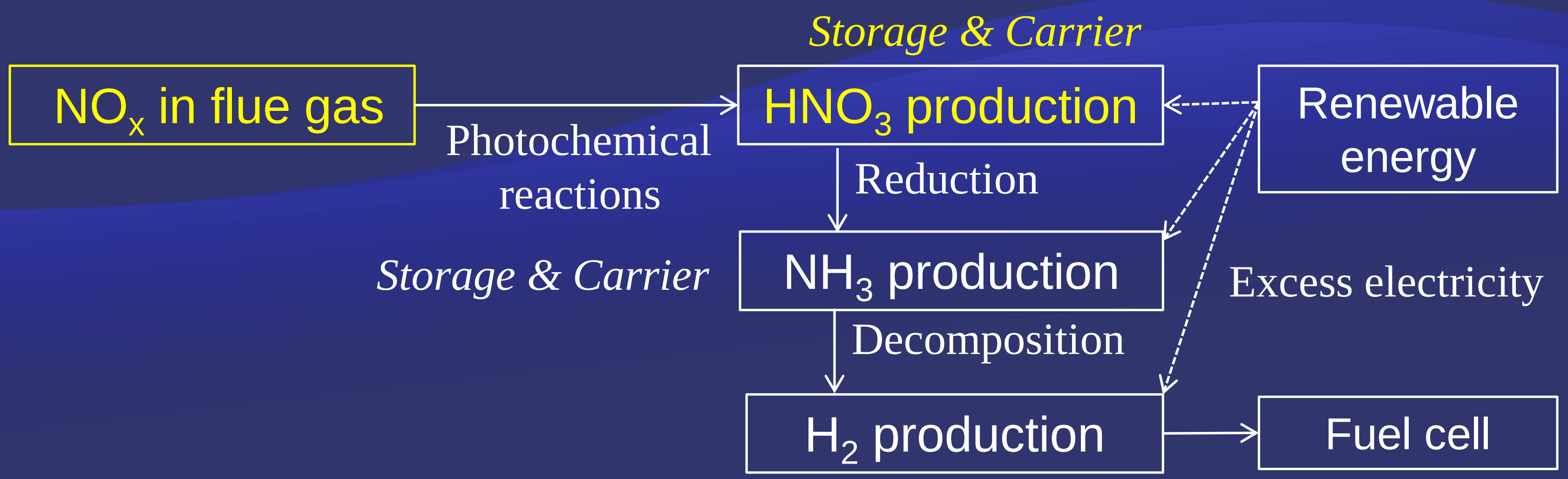

Storage & Carrier

NO_x in flue gas

Photochemical reactions

HNO_3 production

Renewable energy

Reduction

Storage & Carrier

NH_3 production

Excess electricity

Decomposition

H_2 production

Fuel cell

Fig.3 Proposed energy storage and carrier system.

This system has:

1) nitric acid production from NO_x by photochemical reactions,
2) ammonia production from HNO_3 by reduction,
3) hydrogen production by ammonia decomposition.

Technical advantages are:

High efficiency production for HNO_3, NH_3, and H_2.

These reactions are low temperature reactions.

Current Research Topic

Nitric acid production from NO_x by photochemical reactions at room temperature and atmospheric pressure.

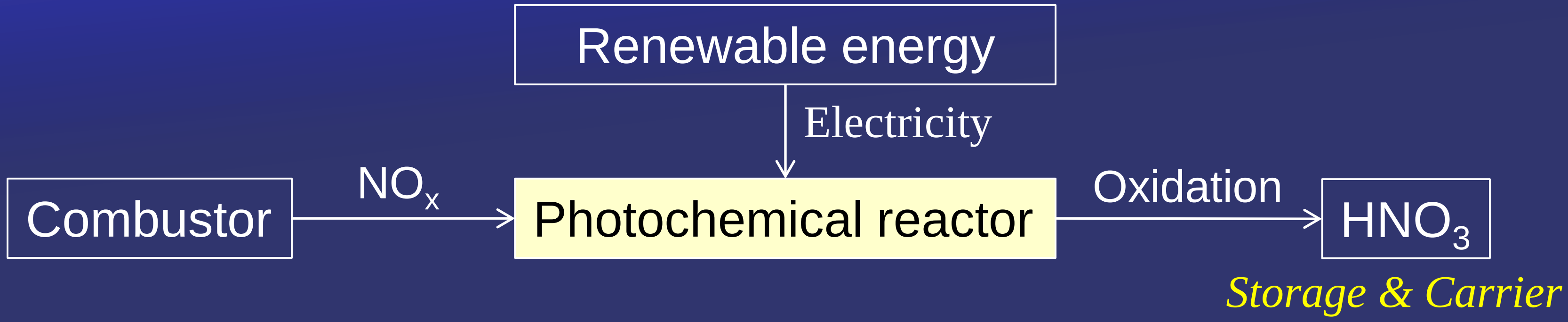

Renewable energy

Electricity

Combustor

NO_x

Photochemical reactor

Oxidation

HNO_3

Storage & Carrier

Fig.4 Current research topic.

<u>Advantages of HNO_3 production from NO_x are:</u>

1) Existing selective catalytic reduction (SCR) is unnecessary.
2) Costly catalyst and deNOx agent (NH_3) for SCR can cut down.
3) HNO_3 easily convert to NH_3 by reduction at low temperature.
4) HNO_3 is available for hydrogen storage and carrier.

Experimental Apparatus

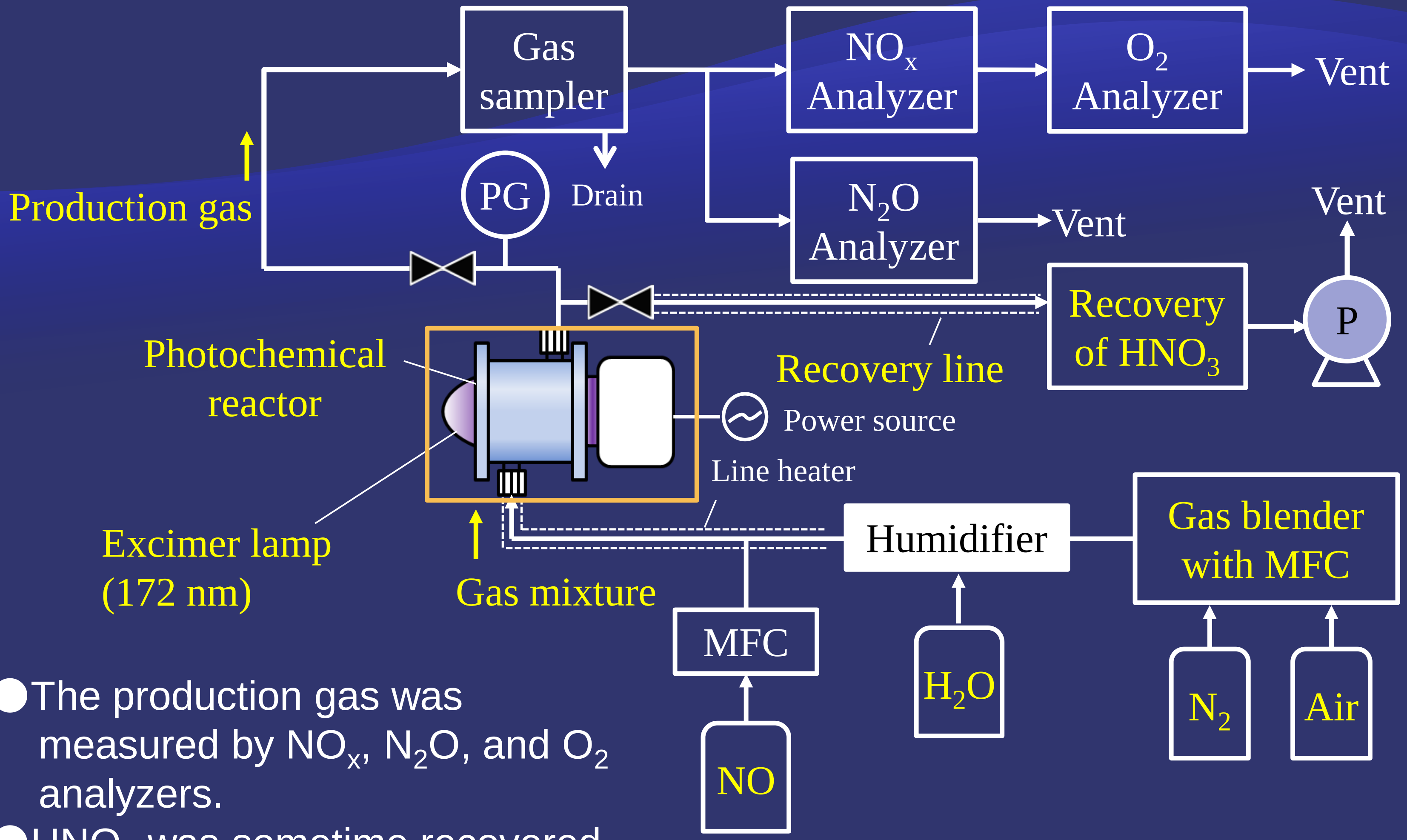

- The production gas was measured by NO$_x$, N$_2$O, and O$_2$ analyzers.
- HNO$_3$ was sometime recovered through the recovery line.

Fig.5 Experimental setup for HNO$_3$ production using vacuum ultra violet.

Details of Photochemical Reactor

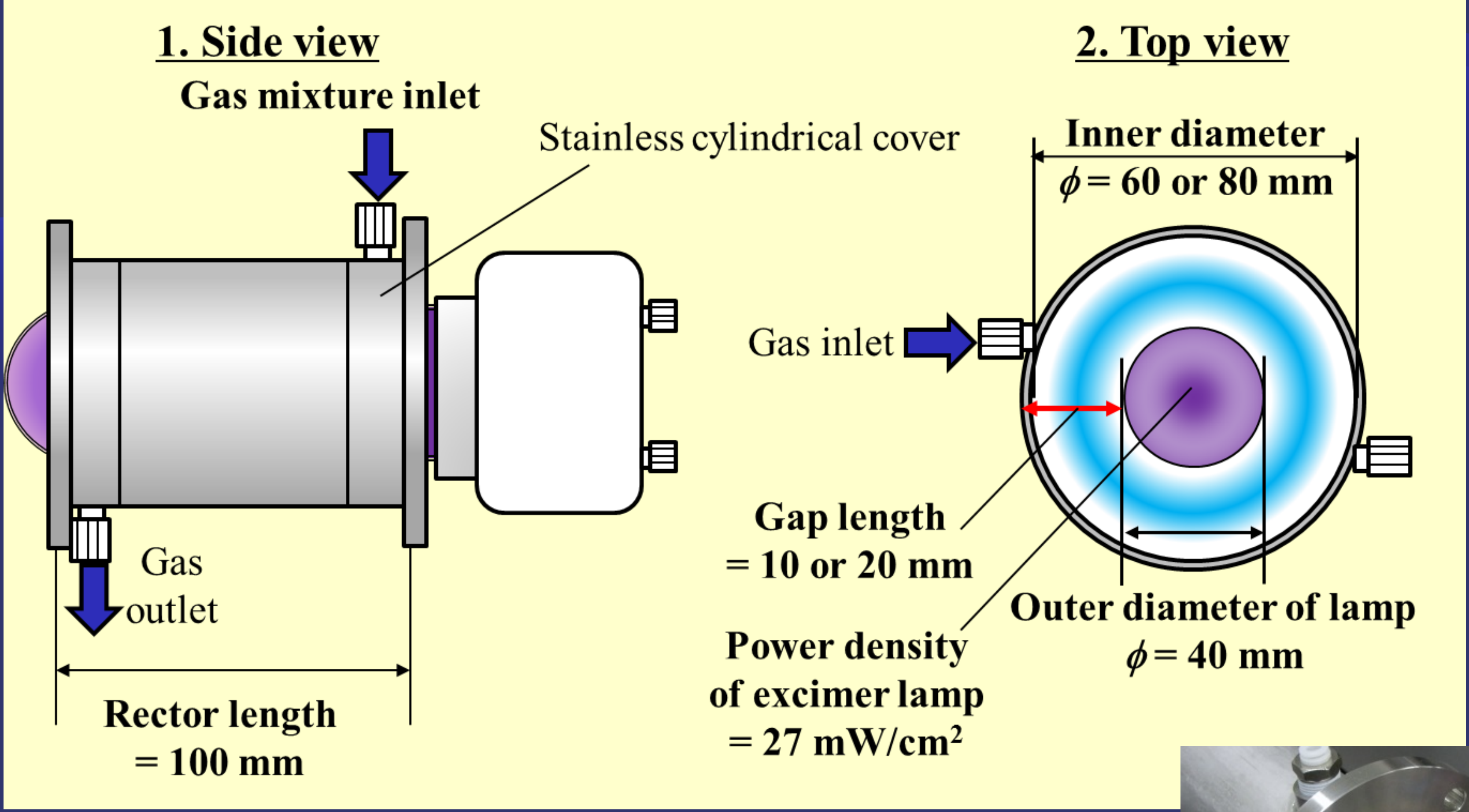

Fig.6 Details of the photochemical reactor

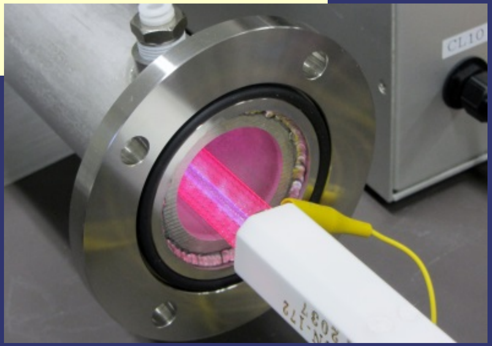

- The photochemical reactor was a coaxial configuration with the excimer lamp.
- The wavelength of excimer lamp is 172 nm.

Experimental Conditions

Table 1 Experimental conditions

Gas composition	$NO/O_2/H_2O/N_2$ gas mixture
Gas flow rate	1.0–5.0 L/min
NO concentration	1500 ppmv
O_2 concentration	0 or 8.3 %
H_2O partial pressure	0–9.5 kPa
Gap length of the reactor	20 or 10 mm
Gas temperature	20°C (room temp.)

Therefore, in this study, four kind of gas composition was examined to investigate reaction paths.

1) $NO/O_2/H_2O/N_2$
2) $NO/O_2/N_2$
3) $NO/H_2O/N_2$
4) NO/N_2

Effect of flow rate on HNO_3 production

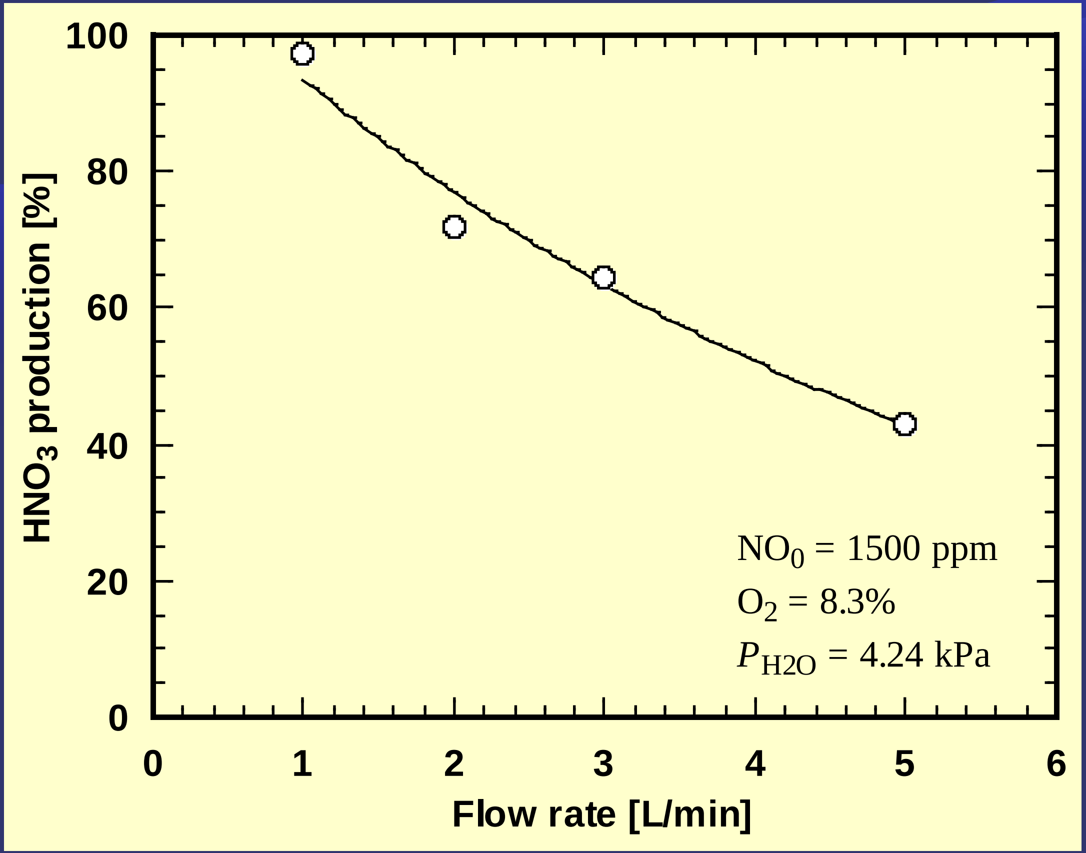

Fig.7 Variation in HNO_3 production with flow rates. ($NO/O_2/H_2O/N_2$ system)

Some reactions are concerned:

As photochemical decomposition,

$H_2O + hv \rightarrow OH + O$ (1)
$O_2 + hv \rightarrow O + O$ (2)
$NO + hv \rightarrow N + O$ (3)
hv is photon energy of VUV.

As gas phase reactions,

$NO + OH + O \rightarrow HNO_3$ (4)
$NO + O \rightarrow NO_2$ (5)
$NO_2 + OH \rightarrow HNO_3$ (6)

These reaction rates depend on the gas residence time. Therefore, HNO_3 production was affected by the flow rates.

The NO conversion to HNO_3 was attained 97% at the flow rate of 1.0 L/min. HNO_3 production was decreased with an increase in the flow rate.

Effect of gas compositions (1)

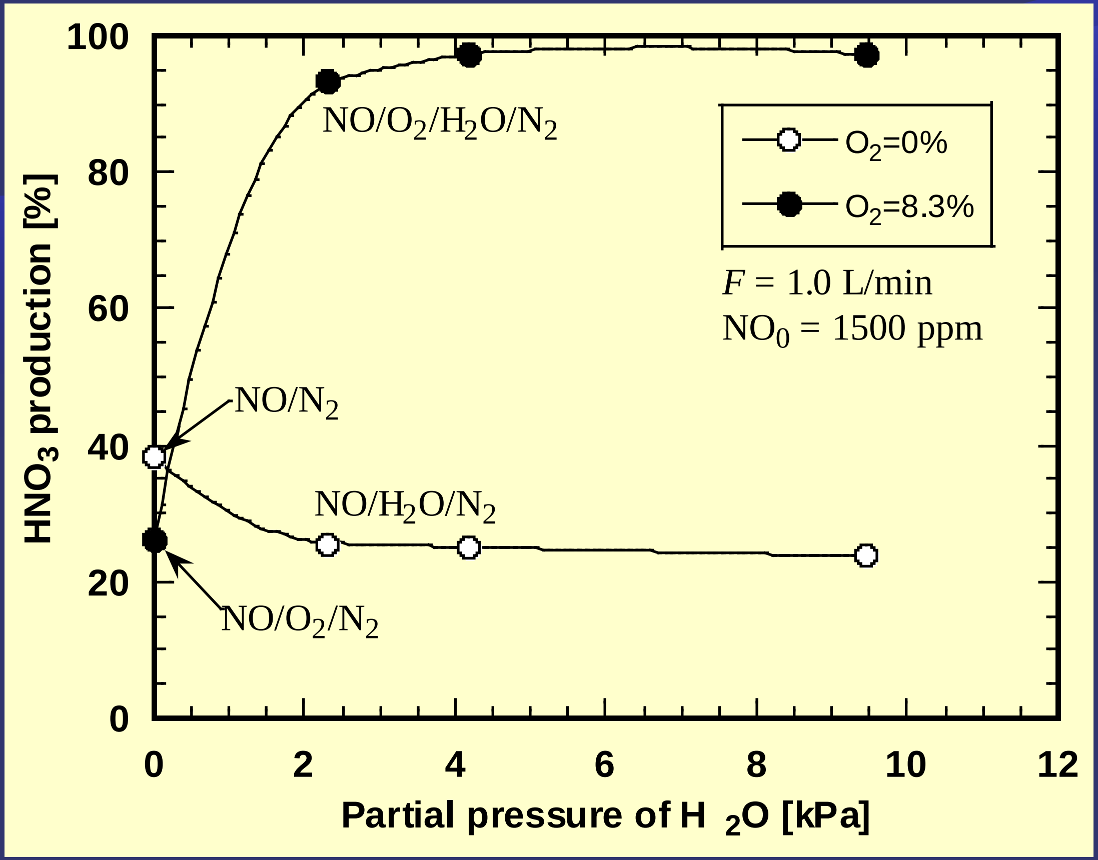

Fig.8 Effect of gas compositions on HNO_3 production as a function of partial pressure of H_2O. White key is 0% O_2, and black key is 8.3% O_2. This figure includes results of four gas system.

The highest HNO_3 production rate was obtained at $NO/O_2/H_2O/N_2$ system.

– Dominant reactions are:

HNO_3 production including

$H_2O + h\nu \rightarrow OH + O$

$O_2 + h\nu \rightarrow O + O$

$NO + OH + O \rightarrow HNO_3$

– Secondary reactions are:

NO reduction

$NO + h\nu \rightarrow N + O$

$N + N \rightarrow N_2$

$O + O \rightarrow O_2$

in NO/N_2 system

HNO_3 production

$H_2O + h\nu \rightarrow OH + O$

$NO + OH + O \rightarrow HNO_3$

in $NO/H_2O/N_2$ system

Effect of gas compositions (2)

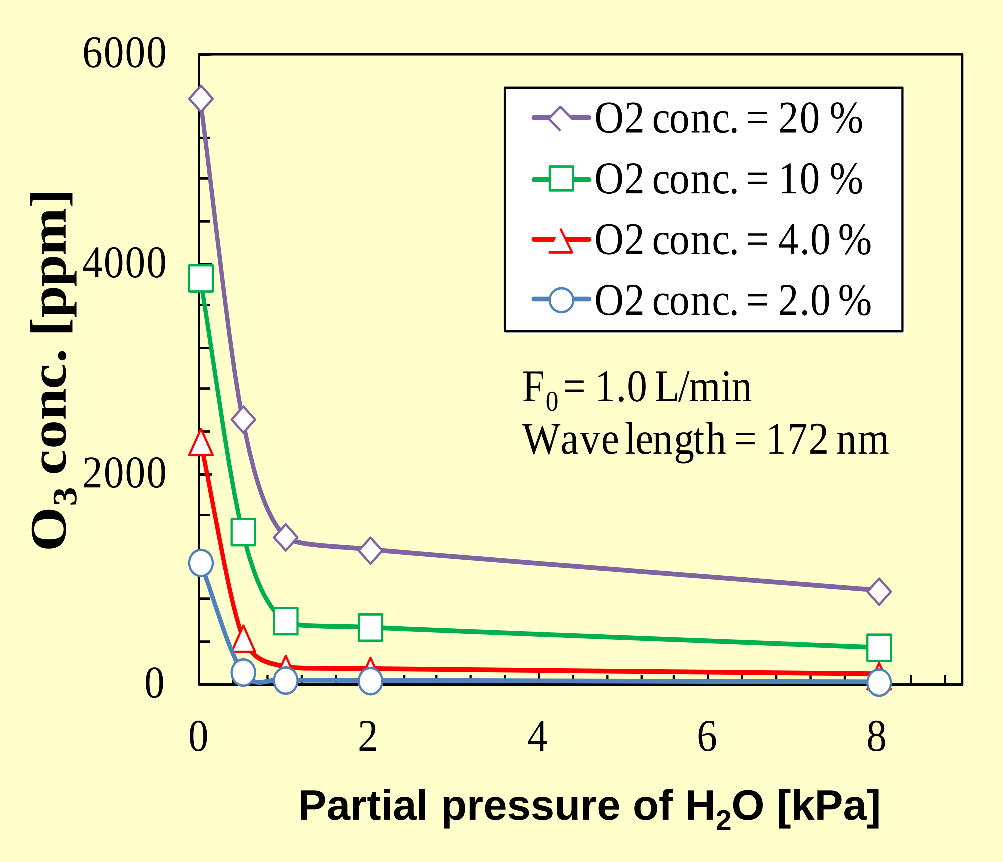

Therefore, in $NO/O_2/N_2$ system, different reactions were concerned:

NO_2 generation

$O_2 + h\nu \rightarrow O + O$

$O_2 + O \rightarrow O_3$

$NO + O_3 \rightarrow NO_2 + O_2$

Fig.9 Behavior of ozone generation as a function of partial pressure of H_2O. Parameter is O_2 concentrations.

Ozone was generated in $NO/O_2/N_2$ and $NO/O_2/H_2O/N_2$ system.

Ozone concentration was decreased with an increase in H_2O concentrations.

Key Reactions of HNO_3 production

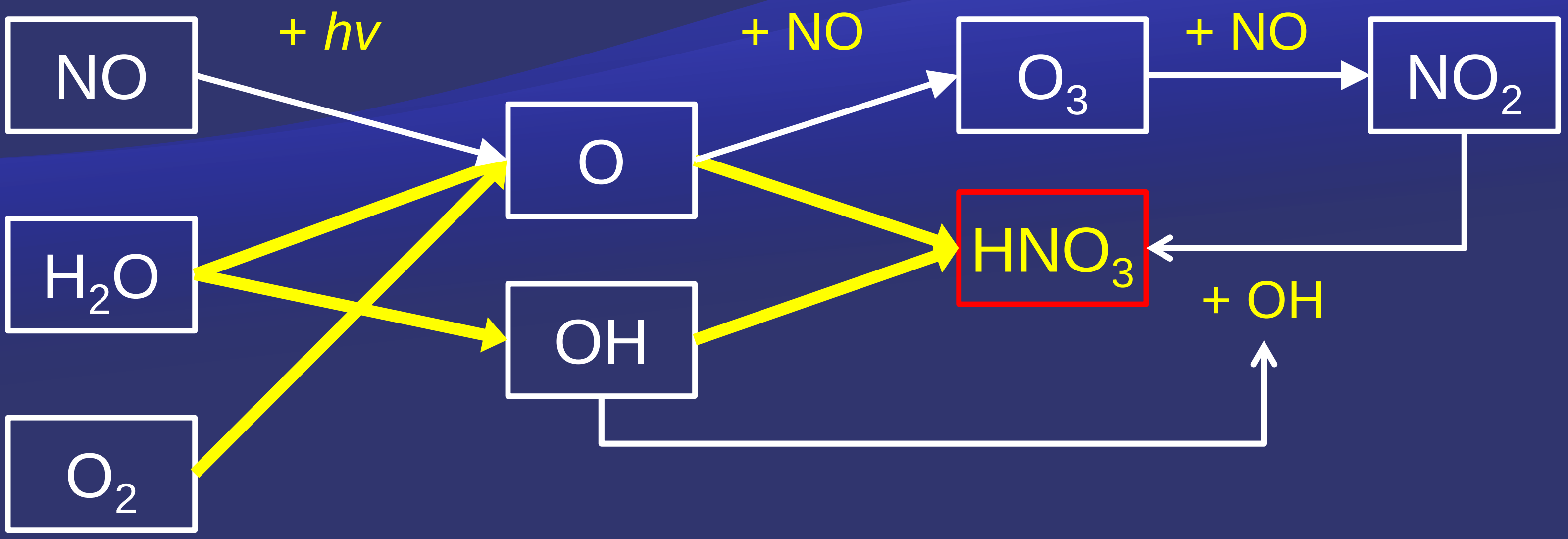

Fig.10 Estimated reaction paths in photochemical reactions for $NO/O_2/H_2O/N_2$ system.

There are three key reactions:

1) O and OH radical generation by photochemical decomposition
2) Radical reactions with NO
3) NO_2 generation by O_3 and NO reaction.

Dominant reactions of HNO_3 production is radical reactions with NO, therefore, HNO_3 production was occurred at low temperature, because activation energy = 0 in radical reactions.